Microbiome

RESEARCH

Open Access

Multiomics insights into rumen microbiome and function in grazing lambs: implications for nutrient absorption and grassland sustainability

Xiuhua Ma[1†], Bing Wang[1†], Minle Xu[2], Yingjun Zhang[2], Nan Liu[2], Li Teng[1], Zhen Li[1], Huan Yang[1], Ximei Xie[1], Bo Zhang[1], Zhi Wang[1], Yuting Wang[1], Jiaguan Liu[1], Jie Bao[1] and Hailing Luo[1*]

Abstract

Background The center of sustainable development of grassland husbandry is the balance between forage intake and growth characteristics of animals, and one of the keys to restricting the conversion efficiency of forage intake is the digestibility of forage produced by rumen microorganisms. Thus, the interaction between grass intake and rumen microbial fermentation is a key driver of both ruminant productivity and grassland ecosystem health. However, interactions between grass species, supplementary feeding, rumen microbiome, and rumen epithelium function, remain poorly understood.

Results We employed metagenomic and metatranscriptomic analyses, coupled with single-cell RNA sequencing (scRNA-seq) of rumen wall and serum metabolomics, to investigate how the rumen microbiome regulates grass intake and host metabolism. In a two-factor (grazing intensity and concentrate supplementation) experiment with 72 lambs, supplementary feeding under moderate grazing increased dry matter intake but decreased grass consumption of *Artemisia tanacetifolia*. These shifts correlated with contrasting trends between metagenomic and metatranscriptomic profiles of *Lachnospiraceae*. scRNA-seq revealed an increased abundance of basal cells (BCs), terminally differentiated keratinocytes (TDKs), and differentiated keratinocytes (DKs) in the supplemented group, with solute carrier genes (e.g., *SLC16A1*) involved in short chain fatty acids (SCFAs) transport enriched in basal cells. We also identified interactions between the rumen microbiome and host epithelial cells, influencing gene expression and localization, which in turn mediated the animal serum nutrient metabolism, particularly in B vitamin, bile acids, and amino acids.

Conclusions Our study identified key microbiome and epithelial cell subtypes involved in grass digestion and SCFAs metabolism in the rumen. This novel link between ruminal microbial function, epithelial cell cluster-based genes, and host metabolism provides critical insights into mechanisms underlying the interaction between grass intake and supplementary feeding for optimizing ruminant management strategies in sustainable grazing systems.

Keywords Lambs, Grazing, Grass intake, Metagenomic, Metatranscriptomics, Single-cell RNA sequencing

†Xiuhua Ma and Bing Wang contributed equally to this work.

*Correspondence:
Hailing Luo
luohailing@cau.edu.cn
Full list of author information is available at the end of the article

Background

China's vast grassland area, comprising approximately 12% of the global total, ranks among the largest in the world. The Mongolian Plateau grassland ecosystem is particularly noteworthy, with the Inner Mongolia Autonomous Region alone containing nearly one-third of China's grasslands [1]. However, the ongoing degradation of these natural ecosystems has led to the increasing adoption of a "grazing plus supplementation" ruminants feeding strategy for the sustainable development of these pastoral areas. This approach, which combines grazing with supplementary feeding, has been shown to enhance both pasture productivity and sheep production by altering foraging behavior [2, 3]. Moreover, this combined feeding strategy positively exhibited a higher loin eye area, crude protein content, and fatty acid profile in sheep compared to indoor feeding [4], largely due to the differences in rumen microbial structure and function resulting from grazing and fresh forage intake, which ultimately influenced the production and absorption of rumen microbial metabolites [5–7].

The rumen microbiome is fundamental to the digestion process in ruminants, playing a vital role in breaking down grass fiber. This complex microbial community includes bacteria, protozoa, fungi, and archaea and within the host they exist in varying abundance and diversity. Many microorganisms, in particular fibrolytic bacteria, convert complex plant polysaccharides into short chain fatty acids (SCFAs), microbial proteins, and vitamins, which are then absorbed through the rumen epithelium and ultimately act on the host's metabolism [8, 9]. By integrating metagenomics and metatranscriptomics, researchers can perform a comprehensive analysis of gene abundance differences between microbial DNA and RNA, offering deeper insights into the functional roles of these microbes [10, 11]. Moreover, the interaction between the host and its microbiome can impact the host's health and behavior [12]. The ruminal epithelium is crucial in this dynamic, serving as the primary site for nutrient absorption and interaction with the microbial community. SCFAs, the main products of microbial fermentation, are absorbed through the keratinized stratified squamous epithelium of the rumen, which can meet up to 70% of the host's daily energy requirements [13]. This epithelium is composed of four distinct cell layers: basal, stratum spinosum, granular, and corium, each with specific functions. Notably, the basal and stratum spinosum cells play a key role in the uptake and metabolism of SCFAs [14, 15]. Each rumen cell layer may have distinct functions and gene expression patterns to optimize the absorption of ruminal metabolites [16]. Single-cell RNA sequencing (scRNA-seq) technology allows for the detailed analysis of tissue heterogeneity, enabling the identification of cell identity, fate, and function. This technology has been applied to enhance our understanding of animal nutrition, health, genetics, and disease models in livestock [17, 18]. The metabolites produced by rumen microbes are absorbed by epithelial cells and enter the bloodstream, supplying nutrients throughout the body and promoting growth and development in the animal [19].

It is well-established that diet and nutrition influence the rumen microbiome, impacting rumen function, metabolism, and overall health [20]. However, the very complex ingestive behavior of grazing animals determines nutrient supply and significantly impacts their performance and feed efficiency, as their short-term forage intake is influenced by both the structure of the forage and the effect of ingested forage on gut fill, which is regulated by the hunger-satiety complex [21]. We hypothesize that the rumen microbiome of lambs mediates their grazing behavior and nutritional metabolism, ultimately influencing host performance and grassland ecological conservation. We used a multiomics approach including rumen metagenomics, metatranscriptomics, metabolomics (both rumen fluid and blood), and single-cell RNA sequencing to explore the mechanisms of symbiotic relationships of grass-rumen microbe-host interactions under grazing plus supplemental feeding systems.

Results

Grazing intensity and supplemental feeding level on lamb performance and feed intake

No significant interaction was observed between grazing intensity and supplemental feeding level on lamb performance and feed intake; however, both factors independently influenced production performance (Table 1) and feed intake (Table 2).

Moderate grazing (MG) significantly increased live weight before slaughter ($P=0.035$), carcass weight ($P=0.008$), and average daily gain (ADG) ($P=0.008$) in lambs compared to heavy grazing (HG). Similarly, high supplementation (HS) significantly improved live weight before slaughter ($P<0.001$), carcass weight ($P<0.001$), and ADG ($P=0.001$) compared to low supplementation (LS) and no supplementation (Table 1). In terms of dietary intake, MG significantly enhanced dry matter intake (DMI) ($P=0.003$), forage intake ($P=0.001$), total organic matter intake ($P=0.003$), digestible crude protein intake ($P=0.026$), neutral detergent fiber intake ($P=0.001$), and acid detergent fiber intake ($P=0.002$) compared to HG. HS further improved DMI ($P<0.001$), total organic matter intake ($P<0.001$), and digestible crude protein intake ($P < 0.001$) compared to LS and no supplementation. LS also showed improvements in the above parameters compared to no supplementation ($P<0.001$). Notably,

Table 1 Effects of different grazing intensities and supplemental feeding levels on animal production performance

Items	Moderate grazing (MG)			Heavy grazing (HG)			SEM	Grazing intensity		Supplementary feeding levels			*P* value		
	NS	LS	HS	NS	LS	HS		MG	HG	NO supplement	LS	HS	Grazing	Supplementation	Interaction
Live weight before slaughter, kg	28.53	32.07	39.61	28.62	39.07	34.39	0.629	33.4	30.69	28.58^{b}	30.57^{b}	37.00^{a}	0.035	< 0.001	0.231
Carcass weight, kg	11.66	14.52	17.99	11.69	12.52	14.5	0.329	14.72	12.9	11.68^{b}	13.52^{b}	16.25^{a}	0.008	< 0.001	0.097
Slaughter rate, %	40.61	45.26	44.75	41.24	40.49	43.7	0.62	43.54	41.81	40.93	42.87	44.23	0.168	0.099	0.198
ADG, g/day	146.98	166.88	207.12	103.1	137.54	172.54	6.273	173.66	137.72	125.03^{b}	152.21^{b}	189.83^{a}	0.008	0.001	0.892

The above indicators were analyzed using linear mixed modeling (IBM SPSS 26.0, USA), with a significance level of $P < 0.05$.Peer data shouldered with the same lowercase letter indicates a non-significant difference ($P > 0.05$), and different lowercase letters indicate a significant difference ($P < 0.05$). *NS* no supplement, *LS* supplementary feeding at the level of 1% of body weight, *HS* supplementary feeding at the level of 2% of body weight, *SEM* standard error of the mean. I denotes the interaction effect of Grazing and Supplementation

Table 2 Effects of different grazing intensities and supplemental feeding levels on feed intake

Items	Moderate grazing (MG)			Heavy grazing (HG)			SEM	Grazing intensity		Supplementary feeding levels			*P* value		
	NS	LS	HS	NS	LS	HS		MG	HG	NO	LS	HS	Grazing	Supplementation	Interaction
DMI	1012.98	1191.48	1338.95	804.48	1008.13	1161.02	29.171	1181.14	991.21	908.72^{c}	1099.80^{b}	1249.98^{a}	0.003	< 0.001	0.974
Forage intake	1012.98	936.48	803.95	804.48	753.13	664.35	24.073	917.8	740.65	908.72^{a}	844.80^{a}	734.15^{b}	0.001	0.02	0.84
Total organic matter intake	944.78	1106.13	1248.74	750.22	932.97	1082.74	27.082	1099.88	921.98	847.51^{c}	1019.55^{b}	1165.74^{a}	0.003	< 0.001	0.975
Digestible crude protein intake	84.28	128.67	165.84	73.75	117.09	155.12	2.338	126.26	115.32	79.01^{c}	122.88^{b}	160.48^{a}	0.026	< 0.001	0.995
Neutral detergent fiber intake	682.5	692.35	678.82	537.3	546.18	560.34	18.81	684.56	547.94	609.9	619.26	619.58	0.001	0.972	0.944
Acid detergent fiber intake	381.36	364.16	336.64	295.83	291.07	275	10.618	360.72	287.3	338.59	327.61	305.82	0.002	0.449	0.9

The above indicators were analyzed using a linear mixed modeling (IBM SPSS 26.0, USA), with a significance level of $P < 0.05$. Peer data shouldered with the same lowercase letter indicates a non-significant difference ($P > 0.05$), and different lowercase letters indicate a significant difference ($P < 0.05$). *NS* no supplement, *LS* supplementary feeding at the level of 1% of body weight, *HS* supplementary feeding at the level of 2% of body weight, *SEM* standard error of the mean. I denotes the interaction effect of Grazing and Supplementation

HS significantly reduced forage intake compared to LS and no supplementation, while LS reduced forage intake compared to no supplementation ($P=0.020$) (Table 2). Based on these results, the MGHS (Moderate Grazing + High Supplementation) and MGNS (Moderate Grazing + No Supplementation) groups were selected for further analysis.

Grazing with supplementary feeding on grass intake and rumen fermentation characteristics

Moderate grazing with high supplementation (MGHS) increased total feed intake (adjusted $P=0.009$) while reducing forage dry matter intake (adjusted $P=0.019$) and the consumption of dominant forage species (Fig. 1A). MGHS reduced the proportion of *Artemisia tanacetifolia* in the diet (adjusted $P=0.012$) (Fig. 1B) and decreased the absolute intake of most grass species (Fig. 1C), none reached significant differences. MGHS increased average daily gain (ADG; adjusted $P=0.004$), pre-slaughter live weight (adjusted $P<0.001$), slaughter rate (adjusted $P<0.001$), and carcass weight (adjusted $P<0.001$) (Table S1). The MGHS group exhibited a significant increase in total SCFA concentrations (adjusted $P=0.003$; Fig. 1D), while no significant differences were observed in the relative proportions of individual SCFAs (Table S2), rumen fluid pH, acetate-to-propionate ratio, or ammonia nitrogen concentration (Fig. 1D).

Rumen fluid metabolome in a grass-fed diet, with or without supplement lambs

The OPLS-DA model revealed clear differences between the two groups (Fig. 2A, $Q<0.05$), with 597 upregulated and 35 downregulated metabolites in the MGHS group compared to MGNS. For instance, antioxidants such as 2,6-cyclolycopene-1,5-diol and astaxanthin were significantly increased in MGHS (Table S3, $Q<0.05$). Receiver operating characteristic (ROC) analysis highlighted the top ten up- and downregulated metabolites, visualized via heatmaps. Notably, metabolites such as (3S,3′R,5R,6R)−7′,8′-Didehydro-3,6-epoxy-5,6-dihydro-beta, beta-carotene-3′,5-diol, Lutein 5,6-epoxide, and arthrobactin were increased in MGHS in comparison to MGNS, while 1,2-dioleoyl-sn-glycero-3-phosphate and tetracosanoic acid were increased in MGNS in comparison to MGHS (Table S4, S5, $Q<0.05$). Key pathways enriched for these metabolites included riboflavin and nicotinate/nicotinamide metabolism (Fig. 2B, $P<0.05$), with riboflavin, flavin adenine dinucleotide (FAD), flavin mononucleotide (FMN), nicotinate, nicotinamide, and pantothenic acid significantly increased in MGHS compared to MGNS ($P<0.05$, Table S6).

Rumen microbiome metagenome in a grass-fed diet, with or without supplement lambs

All rumen metagenome sequencing samples yielded 941,372,608 raw reads, with 927,528,928 reads retained after quality control. On average, each sample had 78,447,717 ± 7,854,648 raw reads, of which 77,294,077 ± 7,742,824 reads were retained post-quality control (Table S7). Moderate grazing with supplementary feeding significantly altered rumen microbial composition, though α-diversity was unaffected (Fig. S1A). No significant differences were found between the MGNS and MGHS groups for species richness, as indicated by the Chao1 and Observed species indices; diversity, as indicated by the Shannon and Simpson indices; evenness, as indicated by Pielou's evenness index; and coverage, as indicated by Good's coverage index (Fig. S1A). Principal coordinate analysis (PCoA) revealed distinct clustering between MGHS and MGNS groups (Adonis test, $R^2=0.179$, $P=0.003$) (Fig. 2C). Among dominant phyla, *Actinobacteriota* and *Firmicutes* were more abundant in MGHS, while *Spirochaetota*, *Methanobacteriota*, and *Verrucomicrobiota* were less prevalent (Table S8). *Actinobacteriota* ($P=0.002$), *Firmicutes* ($P=0.004$), were more significantly abundant in MGHS compared to MGNS, while *Verrucomicrobiota* ($P=0.025$) and *Chloroflexota* ($P=0.015$) were lower in MGHS in comparison to MGNS. At the family level, *Lachnospiraceae* ($P=0.048$) and *Muribaculaceae* ($P=0.046$) were significantly more abundant in MGHS compared to MGNS, while *UBA932* ($P=0.004$), *Oscillospiraceae* ($P=0.012$) and *CAG-74* ($P=0.003$) were lower in MGHS in comparison to MGNS (Fig. S1B). Genera analysis showed significant enrichment of *Sodaliphilus* ($P=0.046$) and *CAG-791* ($P=0.024$) in MGHS, while *Cryptobacteroides* ($P=0.043$) and *Limimorpha* ($P<0.001$) were significantly increased in MGNS compared to MGHS (Table S9). Differential analysis revealed *Prevotella* sp900315525 ($P=0.015$) and *Kandleria vitulina* ($P=0.026$) were significantly increased in MGHS in comparison to MGNS, while *Prevotella* sp002449845 ($P=0.004$) dominated in MGNS in comparison to MGHS (Fig. 2E, F).

Carbohydrate-active enzyme (CAZyme) analysis showed that the MGNS group exhibited significantly higher numbers of CBM ($P=0.004$) and PL ($P=0.026$) modules compared to the MGHS group (Fig. 2G). The distribution of these CAZymes varied across different genera, with *Prevotella* and *Cryptobacteroides* showing the highest proportions. Notably, *Prevotella* had significantly higher numbers of carbohydrate binding modules (CBM) and polysaccharide lyases (PL) modules in the MGHS group, whereas *Cryptobacteroides* exhibited higher CBM and PL numbers in the MGNS group (Fig. S2A and B). The top twenty CAZymes revealed six with significant differences

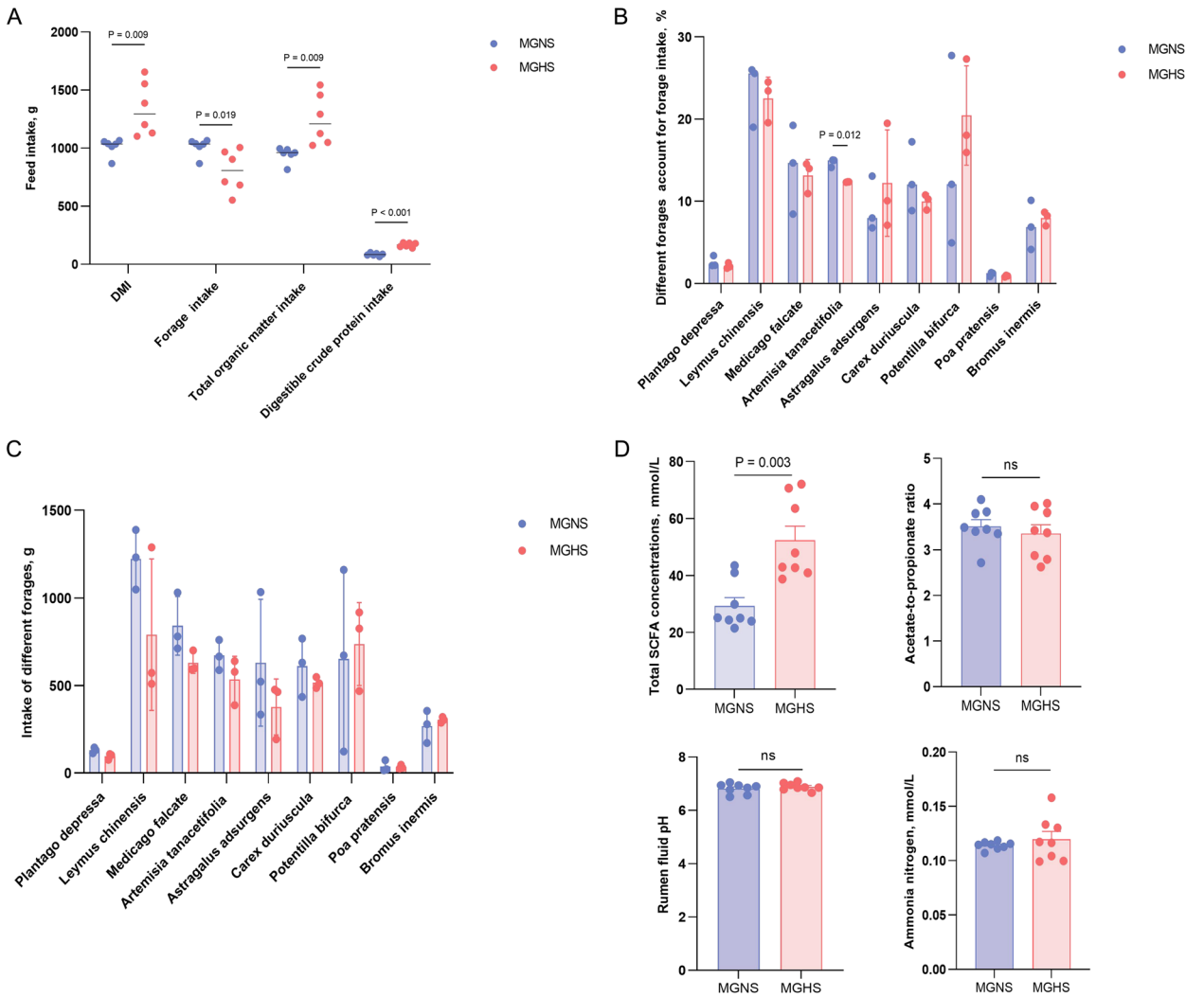

Fig. 1 Grass intake and rumen fermentation characteristics. **A** Differences in dry matter intake (DMI), forage intake, total organic matter, and digestible crude protein between MGHS and MGNS lambs. **B** Different forages account for total forage intake. **C** Intake of different forages. **D** Differences in rumen fermentation

between the two groups: glycosyl transferases 0 (GT0), glycoside hydrolases 0 (GH0), GH25, GH1, GT4, and GT2 (Fig. 2H). Except for GH0, all were more abundant in the MGHS group. The GH25 family includes lysozymes that disrupt β−1,4 glycosidic bonds in cell walls, GH1 is critical for carbohydrate degradation, GT4 participates in sucrose synthesis, and GT2 is involved in cellulose synthesis. The top 50 KOs were selected for differential functional analysis (Fig. 2I). In the MGHS group, KOs related to starch and sucrose metabolism (sucrose-6-phosphatase, K07024; $P=0.002$) were significantly increased in comparison to MGNS. In contrast, the MGNS group exhibited significant higher abundance of KOs associated with carbohydrate metabolism (pyruvate-ferredoxin/flavodoxin oxidoreductase, K03737; $P=0.015$), long-chain acyl-CoA synthetase (simple sugar transport system permease protein, K02057; $P=0.041$), ABC transporters (putative aldouronate transport system substrate-binding protein, K17318; $P=0.009$), and fatty acid metabolism (long-chain acyl-CoA synthetase, K01897; $P=0.041$) compared to MGHS.

Rumen microbiome metatranscriptome in a grass-fed diet, with or without supplement lambs

Rumen metatranscriptome sequencing produced 88,545,103 ± 6,554,982 reads per sample, with 87,294,937 ± 6,472,683 retained after quality control (Table S10). Analysis of the top 20 genera revealed significant differences between the MGHS and MGNS groups. UBA2862 ($P=0.019$), *Limivicinus* ($P=0.004$), and *Fretibacterium* ($P=0.033$) were significantly more abundant in the

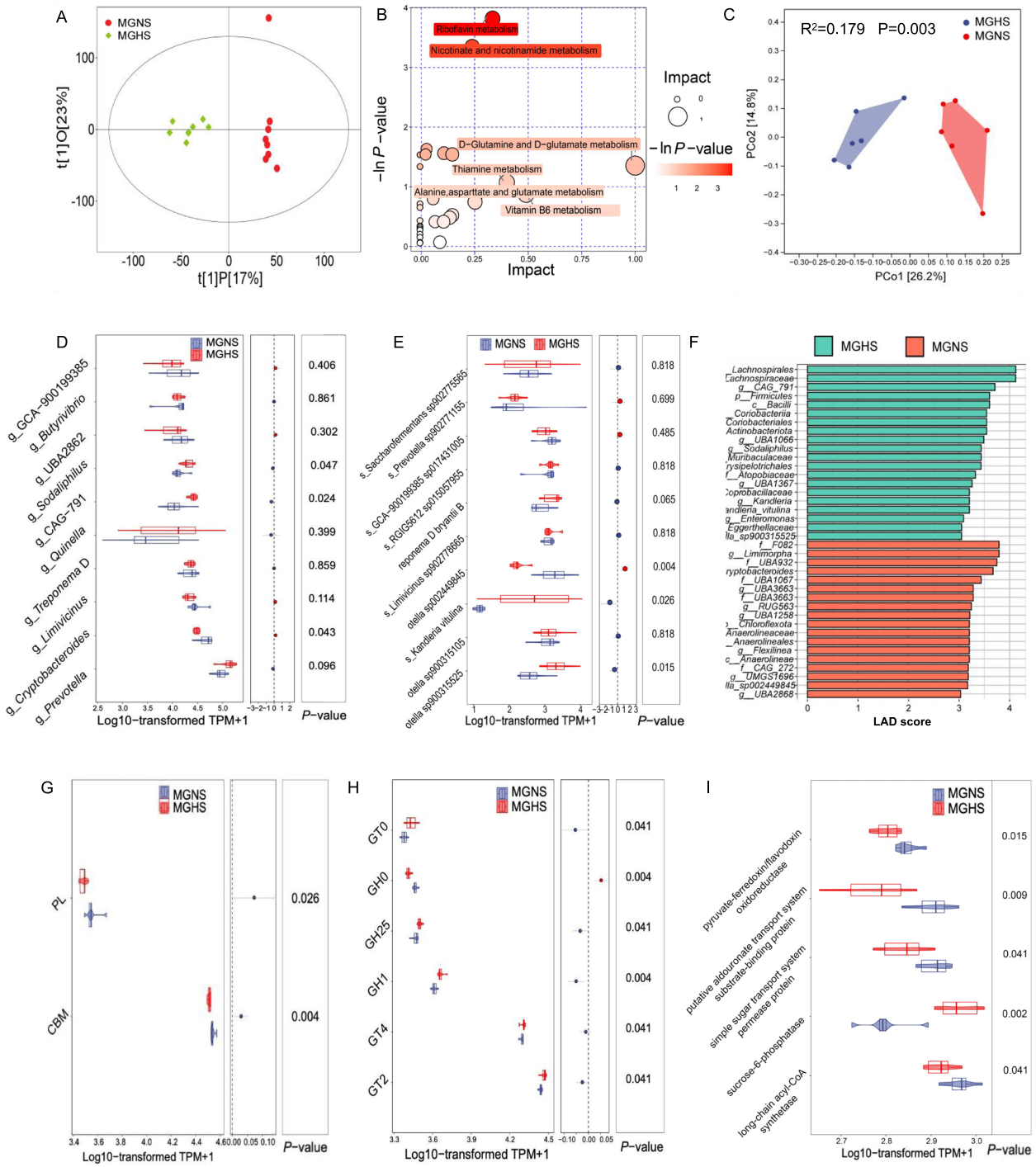

Fig. 2 Metabolomics and metagenomics analysis of rumen microbiome. **A** Score scatter plot of OPLS-DA model between MGHS and MGNS. **B** Metabolic pathway analysis bubble diagram. **C** Principal coordinates analysis (PCoA) of rumen microbes between MGHS and MGNS. **D** The top 10 most abundant genera. **E** The top 10 most abundant species. **F** All significantly different rumen bacterial species. Microbial phyla, order, family, genera, and species were compared using linear discriminant analysis effect size (LEfSe), with LDA score > 3 and *P*-value < 0.05 being considered as significantly different. **G** Differences in class-level CAZyme between MGHS and MGNS lambs. **H** The top 20 CAZyme. Significantly different CAZymes were tested by Wilcoxon with *P*-value of < 0.05. **I** The top 50 KOs for differential functional analysis by the KEGG database

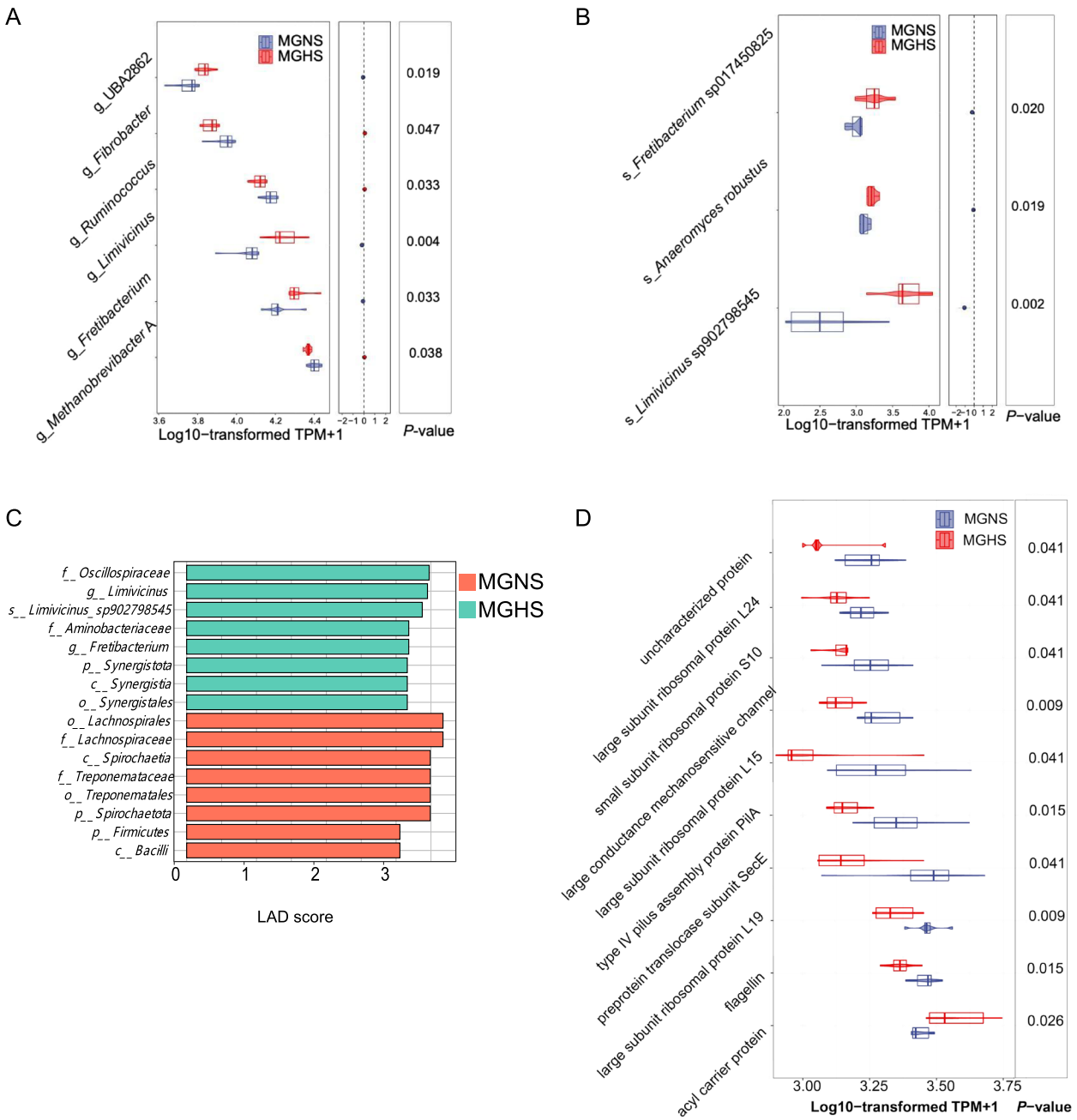

Fig. 3 Meta-transcriptomics of rumen microbiome. **A** Difference of the top 20 genus between MGHS and MGNS lambs. **B** Difference of the top 20 species between MGHS and MGNS lambs. **C** The linear discriminant analysis effect size (LEfSe) analysis showing the different microbial community. **D** The top 50 KEGG orthologys (KOs) in the rumen microbiome with *P*-value < 0.05 were considered as significantly different

MGHS group, while *Ruminococcus* ($P=0.033$), *Fibrobacter* ($P=0.047$), and *Methanobrevibacter A* ($P=0.038$) were more prevalent in MGNS (Fig. 3A). No significant difference was observed in *Cryptobacteroides* between the groups. At the species level, *Fretibacterium* sp017450825 ($P=0.020$), *Anaeromyces robustus* ($P=0.019$), and *Limivicinus* sp 902,798,545 ($P=0.002$) were significantly increased in MGHS compared to MGNS (Fig. 3B). LEfSe analysis confirmed the differences of these microbes (Fig. 3C). Among the top 50 KEGG orthologs (KOs), the abundance of large subunit ribosomal protein L19 (K02884) ($P=0.009$) and flagellin (K02406) ($P=0.015$) significantly increased in MGNS in comparison to MGHS, while acyl carrier protein

(K02078) ($P=0.026$), involved in antibiotic and secondary metabolite biosynthesis, significantly increased in MGHS in comparison to MGNS (Fig. 3D).

We conducted single-cell analysis of rumen epithelium from two treatment groups, dissociating tissues and isolating live single cells for genomic profiling (Fig. 4A). A total of 7131 single cells were sequenced, yielding an average of 1921 genes per cell. After quality control, 6573 cells were retained, with a median of 1889 genes per cell. Using t-Distributed Stochastic Neighbor Embedding (tSNE), we identified 13 distinct cell clusters, showing significant overlap between the two groups (Fig. 4B, C). Clusters 1 and 4 were basal cells (BCs) expressing markers *KRT15*, *KRT5*, *HSD17B2*, and *COL17A1*. Clusters 2 and 3 expressed differentiated keratinocyte (DK) markers *DSC1*, *DSG1*, and *SPINK5*, while cluster 10 represented terminally differentiated keratinocytes (TDKs) expressing *S100A8*, *KRT17*, *KRT36*, and *SFN*. Clusters 21 and 18 were mast cells, clusters 0, 17, and 20 were T cells, and clusters 9, 11, and 14 were macrophages. Cluster 6, expressing *GNLY*, *CTSW*, *KLRK1*, *CCL5*, and *NKG7*, was identified as natural killer cells (Fig. 4D). Notably, genes involved in SCFAs transport, including *SLC16A1*, *SLC4A9*, *SLC26A2*, *SLC22A23*, *SLC26A3*, and *SLC22A5*, were increased in MGHS compared to MGNS diet. *SLC16A1*, *SLC4A9*, and SLC26A2 were mainly found in BCs, with *SLC4A9* encoding a key SCFAs transporter, while *SLC22A23*, *SLC26A3*, and *SLC22A5* were detected in DKs (Fig. 4D).

MGHS compared to MGNS diet treatment increased the proportion of epithelial cells (BCs up by 2.53%, DKs by 7.11%, TDKs by 1.95%) and decreased immune cells (T cells down by 8.83%, macrophages by 2.79%) (Fig. 4E). There were more upregulated genes in rumen epithelium cells in the MGHS-fed lambs (Fig. 4 F), with 1109, 1025, and 666 genes upregulated in BCs, DKs, and TDKs, respectively (Fig. 4G). KEGG analysis showed BCs were enriched in pathways related to oxidative phosphorylation, branched-chain amino acid degradation, and fatty acid metabolism (Fig. 4H). DKs were also linked to oxidative phosphorylation (Fig. S3A), while TDKs were involved in terpenoid backbone biosynthesis, Th1/Th2 cell differentiation, and thyroid hormone signaling (Fig. S3B).

Serum metabolomics in a grass-fed diet, with or without supplement lambs

Non-targeted metabolomics analysis revealed significant metabolic differences between the MGHS and MGNS groups, as indicated by the OPLS-DA model (Fig. 5A). The differentially annotated metabolites were classified into 21 categories, with lipids (22.4%), organoheterocyclic compounds (18.1%), and benzenoids (11.7%) being the most abundant (Fig. S4; $Q<0.05$). A total of 693 metabolites were significantly upregulated and 38 downregulated in MGHS compared to MGNS (Fig. 5B; Table S11; $Q<0.05$). ROC analysis identified key metabolites distinguishing the groups, with 4-acetamidophenol sulfate, dhurrin, and benzoic acid enriched in MGHS, while phytanic acid, chlorpropamide, and pantothenic acid were elevated in MGNS (Fig. 5C; Table S12–13; $Q<0.05$).

Pathway analysis highlighted significant differences in pantothenate and CoA biosynthesis ($P=0.040$) and phenylalanine, tyrosine, and tryptophan biosynthesis ($P=0.040$). Pantothenic acid was increased in MGNS compared to MGHS, whereas L-valine, alpha-ketoisovaleric acid, L-phenylalanine, and L-tyrosine were elevated in MGHS compared to MGNS (Fig. 5D; Table S14, $P<0.05$). Additionally, 19 bile acids, including allocholic acid ($Q<0.05$), ursocholic acid ($Q<0.05$), and alpha-muricholic acid ($Q<0.05$), glycocholic acid ($Q<0.05$), glycochenodeoxycholic acid ($Q<0.05$), chenodeoxycholic acid ($P<0.05$), hyocholic acid ($Q<0.05$), were significantly increased in the MGHS group (Fig. 5E; Table S14).

Discussion

This study highlights the rumen microbiome-epithelium crosstalk mechanism underlying the impact of supplementary feeding on grass intake in lambs under grazing conditions (Fig. 6). Supplementation led to notable changes in grass intake and host metabolism, as evidenced by variations in forage intake and blood metabolome profiles, which was also likely associated with the alterations in the rumen microbiome. These changes were identified using integrative metagenomics, meta-transcriptomics, and single-cell transcriptomics. Concentrate supplementary feeding resulted in a marked increase in dry matter intake, total organic matter intake, and digestible crude protein intake, while simultaneously reducing

(See figure on next page.)

Fig. 4 Single-cell map of the rumen epithelial tissue in lambs. **A** Process flow diagram of the single-cell sequencing strategy employed in this study. **B** and **C** t-SNE map of rumen epithelial single cells showing the 13 cell types of rumen epithelial tissue cells. Cells are colored by cell type. t-SNE map of rumen epithelial single cells between MGHS and MGNS lambs. **D** Dot plot visualization of each cell type in the rumen epithelial single-cell map. Dot size represents the percentage of cells within a cell type, and the color refers to the expression level. **E** Annogram of 13 clusters identified from rumen epithelial tissue in MGHS and MGNS groups by tSNE analysis. **F** t-SNE maps of up-regulated genes. **G** Differences in the number of up-regulated genes in epithelial cells between the MGHS and MGNS groups. **H** KEGG enrichment analysis of the primary function in the BCs cluster

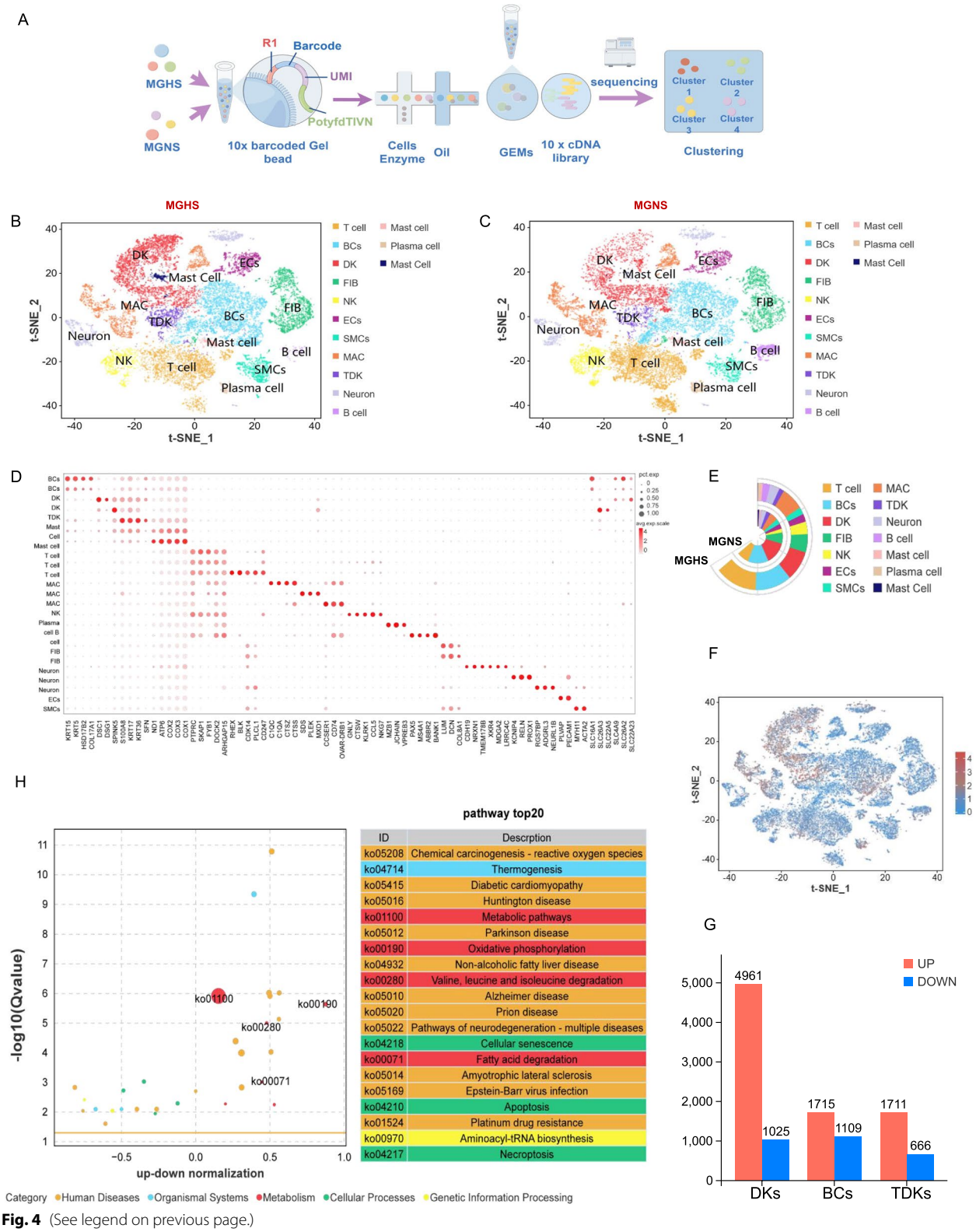

Fig. 4 (See legend on previous page.)

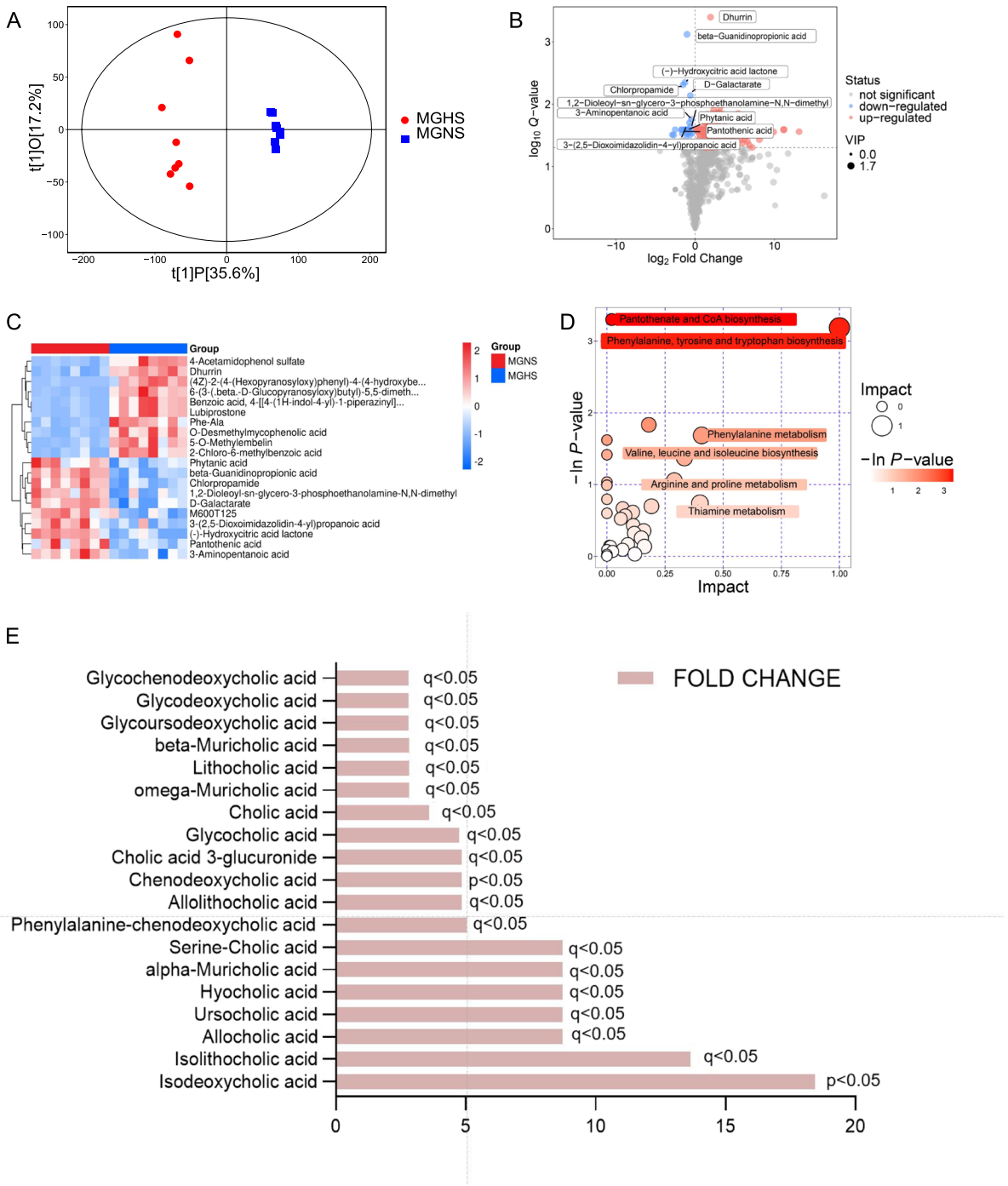

Fig. 5 Serum metabolome of MGHS and MGNS lambs. **A** Score scatter plot of OPLS-DA model between MGHS and MGNS. **B** Volcano plot of differential metabolites between MGHS and MGNS groups. **C** Heatmap of the top ten upregulated and downregulated metabolites based on ROC analysis. **D** Metabolic pathway analysis bubble diagram of basal cells. **E** Serum bile acids that differ significantly between MGHS and MGNS groups (fold change calculated as MGHS/MGNS)

grass intake. This is consistent with previous research indicating that appropriate levels of concentrate supplementation enhance dietary nutrient intake [22]. Similarly, concentrate supplementation reduced forage intake but increased total feed intake and dry matter digestibility, as observed in dairy cows [23] and lambs fed low-protein hay [24]. Despite enhanced nutrient intake, reduced forage consumption likely resulted from accelerated rumen

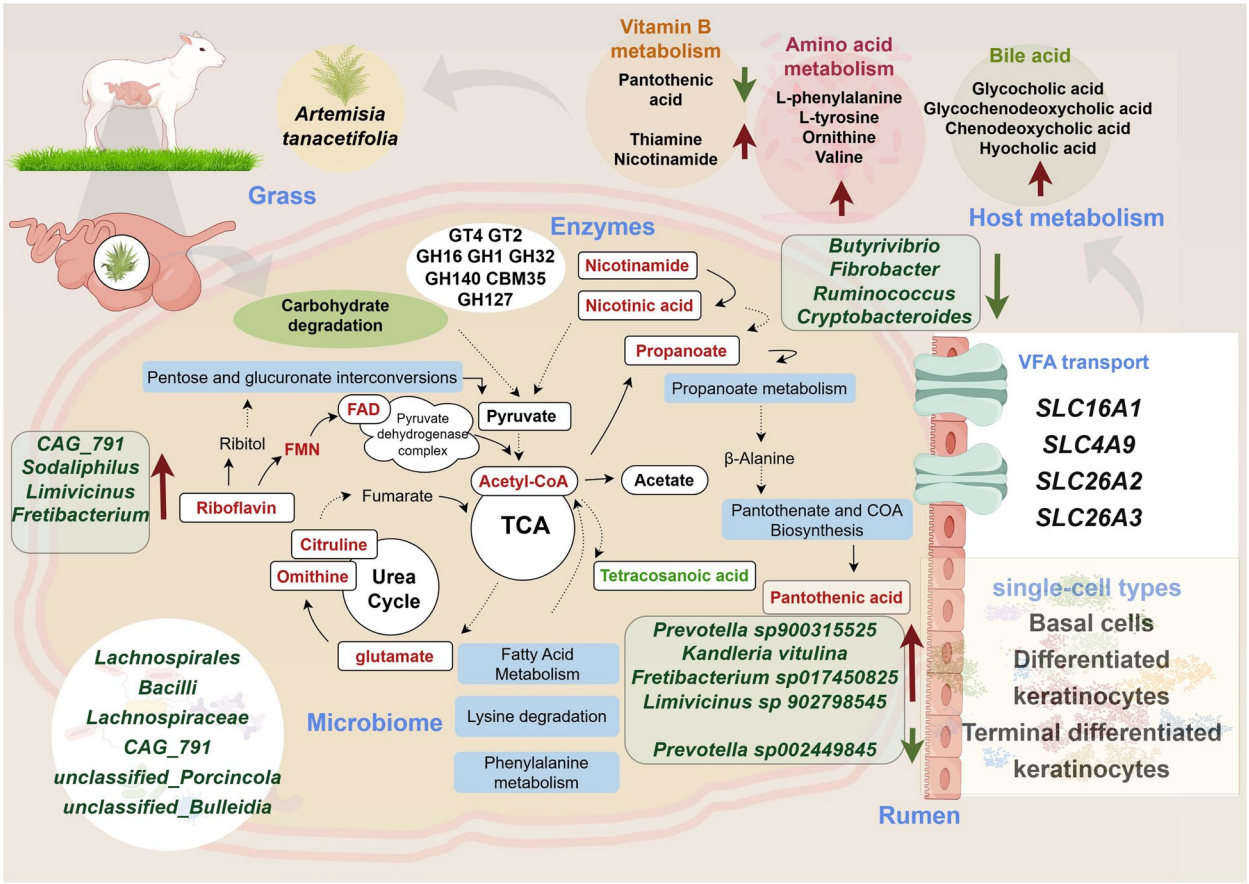

Fig. 6 Overview of putative grass-microbiome-rumen crosstalk pathways in China Mongolian plateau lamb grazing plus concentrate supplementary feeding system. The figure illustrates the potential process by which high expression of the rumen microbiome involved in microorganism and CAZyme genes intervened by concentrate and grass leads to carbohydrate degradation into TCA cycle, urea cycle, propionate metabolism, and pantothenate biosynthesis in the rumen. This promotes a shift in rumen epithelial cells specific cell types and the target cell-related SCFAs transport function, and then interacted with host serum B vitamin metabolism, amino acids metabolism, and bile acid pool. Candidate microbes, metabolites, and host genes are highlighted by arrows and ovals of different colors. This figure was drawn by Figdraw (ID: AARPO93483)

passage of nutrient-dense feeds, which limited rumen filling and triggered early satiety via vagus nerve signaling [25, 26]. The reduction in grass intake indicated that concentrate has improved nutrient profile in comparison to forages in general.

The study also observed that the ingestive proportion of *Artemisia tanacetifolia* was reduced after concentrate supplementation. Artemisia species have been reported as indicators of grassland degradation [27], which demonstrates that supplementary feeding under the current grazing conditions could alter the lambs' dietary preferences for grass. It further suggests that supplementary feeding may reduce the abundance of *Artemisia tanacetifolia* in grasslands while promoting the growth of more nutritious forage species, thereby potentially mitigating grassland desertification [28].

This rise in SCFAs, particularly propionic acid, indicates enhanced microbial activity and energy availability for the host, potentially improving overall productivity and health [29]. The study also found that rumen fluid B vitamins were changed by different grazing pattern, with increased the synthesis of riboflavin, nicotinamide, and nicotinic acid, under the concentrate intervention. Pantothenic acid is crucial for metabolism as it is a key component of coenzyme A and acyl-carrier protein [30]. We also found the decreased serum pantothenic acid under the concentrate intervention. Thus, the concentrate supplementation might have adverse effects on grazing lamb production. It was reported that increasing dietary nonfiber carbohydrate content increased ruminal apparent synthesis of nicotinic acid, nicotinamide, niacin, pyridoxal, B_6, and folic acid [31], which was similar to the current study showing that the increase abundance

of ruminal FAD, flavin mononucleotide, riboflavin, niacinamide, and nicotinate. The enhanced niacin and nicotinic acid metabolism could achieve anti-inflammatory effects [32], and the disruption of niacin and nicotinamide metabolism could lead to a series of adverse reactions caused by inflammation and oxidative stress [33]. Additionally, the astaxanthin and 2, 6-cyclolycopene-1, 5-diol in the rumen fluid were also increased by concentrate supplementation. The astaxanthin has beneficial antioxidative function in animal nutrition [34], but 2, 6-cyclolycopene-1, 5-diol is a marker of oxidative stress [35]. These results suggest that concentrate supplementation altered B vitamin metabolism and influenced rumen inflammation and oxidative status in a pasture feeding system. However, it remains unclear whether these effects are entirely beneficial or harmful.

Supplementary feeding reshaped both microbial composition and functional dynamics. Specifically, it enriched *Lachnospiraceae*, *CAG-791* and *Sodaliphilus* but suppressed *Cryptobacteroides* and *Limimorpha*. Metatranscriptomic profiling further indicated enhanced activity of fibrolytic taxa (e.g., Limivicinus) [36] and reduced expression of cellulose-degrading genes in *Ruminococcus* [37] and *Fibrobacter* [38]. The *Lachnospiraceae* family, belonging to the phylum *Firmicutes*, is one of the most diverse and abundant bacterial families in the rumen microbiome [39]. The *Lachnospiraceae* families are prominent plant degraders contributing to gut health [40]. This is consistent with findings in pasture-fed cattle, where acetogens from these families and hydrogen-responsive *Bacteroidetes* are prevalent [41]. Additionally, comparisons between cultures with and without hydrogen revealed novel strains of *Lachnospiraceae* that declined in the absence of hydrogen, reinforcing their role as dominant acetogens in the rumen [41]. Studies have suggested that *Lachnospiraceae* tend to be more prevalent in cattle with low feed efficiency [41]. *CAG-791* shows potential for enhancing SCFAs production and promoting host health [42]. *Cryptobacteroides*, another important genus in the rumen microbiome, is known for degrading plant materials to produce SCFAs, which are crucial for ruminant energy [43, 44]. *Cryptobacteroides* also aids in immunomodulation, maintaining gut health [43, 44]. This genus, along with *Prevotella*, was prevalent in the rumen microbiome and influenced by diet and monensin, with implications for carcass traits in beef cattle, particularly carcass weight [36, 45, 46]. Interestingly, under supplementary feeding, certain bacterial taxa, including *Lachnospiraceae*, *CAG_791*, and *unclassified_Porcincola*, exhibited significantly higher abundance in metagenomic analysis but showed the opposite trend in metatranscriptomic analysis (Table S15). *Porcincola*, a strictly anaerobic genus within *Lachnospiraceae*, plays a significant role in the rumen ecosystem [47]. The contrasting trends observed between metagenomic and metatranscriptomic analyses for certain rumen microbes may be attributed to the dynamic changes in the rumen environment under grazing plus supplementation system [48]. These shifts in microbial population dynamics could have long-term implications for rumen health and function [49], influencing not only digestion but also the overall metabolic health of the lamb.

For the rumen microbial function analysis, differential abundance of carbohydrate-active enzymes (CAZymes) and key enzymes underscores their importance for the deconstruction of plant biomass. These enzymes, including glycoside hydrolases (GHs), carbohydrate esterases (CEs), polysaccharide lyases (PLs), glycosyltransferases (GTs), and auxiliary activities (AA) enzymes, along with carbohydrate-binding modules (CBMs), are crucial for carbohydrate-binding activity [50]. Metagenomics analysis revealed differential CAZymes, including GT0, GH25, GH1, GT4, and GT2, contributing to the degradation of easily fermentable carbohydrates in the rumen, all of them except for GT0 were enriched with higher value after the supplementary feeding. The GT4 and GT2 families are related to sucrose and cellulose synthesis, respectively [51]. The GH25 family lysozymes break down cell wall insoluble mucopolysaccharides into soluble glycopeptides [52]. The enriched presence of certain CAZymes and key enzymes in the MGHS group points to their role in carbohydrate degradation and microbial adaptation to diet changes [53]. In contrast, enzymes involved in fiber or cellulose degradation such as GH127 responsible for the depolymerization of hemicellulose [54] were more prominent in the only pasture grazing group (MGNS group). Metatranscriptomic analysis revealed enrichment of CAZymes such as GH16, GH42, and PL9 in the MGHS group. GH16 is a plant cell wall-degrading enzyme, GH42 and PL9 are involved in pectin degradation [55], indicating the complex changed carbohydrate degradation altered by changed grass intake and concentrate supplementation.

The scRNA-seq analysis of rumen tissues from two treatment groups (MGNS and MGHS groups) of lambs provides valuable insights into the cellular diversity and molecular mechanisms underlying rumen epithelial development and keratinization. Our study highlights the complexity of cellular identities within the rumen epithelium, which plays a crucial role in the absorption of SCFAs, meeting 70–80% of the body's energy needs. The rumen epithelium, consisting of four distinct cell layers, presents challenges in understanding nutrient absorption mechanisms. Previous studies using scRNA-seq identified the significance of spiny cells in SCFAs absorption

and revealed 18 distinct rumen epithelial cell types with specific metabolic functions [56, 57]. Among these, a subtype known as the channel-gap-like spinous cell, regulated by IL-17, was found to be the most efficient in absorbing SCFAs in dairy cows [57]. The identification of specific cell clusters with unique gene expression profiles indicates that the rumen epithelium is composed of a heterogeneous population of cells. This heterogeneity is consistent with findings in other epithelial tissues, where cellular diversity is essential for maintaining homeostasis and adaptation in the rumen epithelium [56, 58]. The considerable overlap in cellular composition observed between the treatment groups suggests that, despite distinct regulatory mechanisms, the fundamental cellular makeup of the rumen epithelium remains relatively stable across different conditions. The identification of keratinocyte-like cells within these clusters underscores their importance in maintaining epithelial integrity [59]. In terms of SCFAs absorption, our scRNA-seq data highlight the preferential expression of the SLC gene family in the rumen epithelium. Notably, *SLC4A9* is identified as a likely antiporter [60], while *SLC16A1*, which encodes a basolateral membrane SCFAs/bicarbonate antiporter [60]. The highest expression of *SLC16A1* shows it is also likely involved in the transport of ketone bodies into the bloodstream at the basolateral surface of the rumen epithelium [61]. Although previous studies reported generally low expression of the *SLC21A* and *SLC22A* families in the rumen [60], our findings indicate higher expression of these genes, particularly in the DKs with concentrate supplementation, which enhanced their expression. The increased expression of *SLC16A1*, *SLC4A9*, *SLC26A2*, and *SLC26A3* genes, all of which encode apical anion exchangers [60], confirms their role in acetate uptake. The integrative effects of different dietary components result in changes to both the chemical environment of rumen SCFAs and the physical abrasiveness of the diet [62, 63]. Thus, our scRNA-seq data provide a valuable framework for understanding the cellular dynamics of rumen epithelial development in response to grass intake and supplementary feeding.

In this study, we observed an enrichment in the biosynthesis pathways of phenylalanine, tyrosine, and tryptophan, along with increased serum concentrations of L-phenylalanine and L-tyrosine under high supplementary feeding. These findings are consistent with previous studies in beef steers fed a high-corn diet and in the rumen fluid of dairy cows fed a high-concentrate diet [64, 65]. Phenylalanine and tyrosine are precursors to important neurotransmitters and metabolic intermediates. Specifically, tyramine, a decarboxylation product of tyrosine, serves as the biological precursor of octopamine, which functions as a neurotransmitter in invertebrates [66]. Interestingly, low levels of tyramine have been linked to a pro-inflammatory state associated with metabolic syndrome [67]. This underscores the broader relevance of amino acid metabolism in systemic health. We also noted changes in the peripheral plasma levels of homovanillic acid, a metabolite of dopamine, which is often used as an indicator of central nervous system dopamin*ergic* activity [68]. The metabolism of fatty acids was further emphasized by the observation that the content of phytanic acid in milk was positively correlated with dietary phytol intake [69]. Phytanic acid is derived from phytol through enzymatic activity by rumen bacteria [70], illustrating the complex interactions between diet, microbiota, and host metabolism.

The observed changed serum bile acid metabolism in response to supplementary feeding aligns with our previous research in sheep, which identified altered bile acid metabolism-related pathways in the liver under a high-concentrate diet [71]. Specifically, our findings showed increased serum concentrations of 19 bile acids by concentrate supplementary feeding, like previous studies in dairy cows [72]. While this study provides valuable insights into the effects of concentrate supplementation on the rumen microbiome, forage intake, and host metabolism, it also highlights the dynamic and transient nature of microbial responses to dietary changes. Further research is needed to fully understand the long-term implications of these changes and the potential interactions between the rumen microbiome, feed intake, and host physiological responses. Addressing these aspects will be crucial for developing sustainable and effective nutritional strategies in grazing ruminant production systems.

Conclusion

This study demonstrates that supplementary feeding profoundly reshapes the grazing lamb eating habits and metabolic processes, primarily by modulating the rumen microbiome. Supplementary feeding increased dry matter intake while reducing grass consumption and altering the composition of grass species. Selective feeding behavior, driven by enhanced nutritional density, led to a marked decline in species such as *Artemisia tanacetifolia*. These grazing model shifts were associated with changes in the contrasting trends observed between metagenomic and metatranscriptomic analyses for certain rumen microbes such as of *Lachnospiraceae*, which was attributed to the dynamic changes in the rumen environment intervened by supplementary feeding. Additionally, the changes of rumen microbiome were associated with the abundance of the rumen epithelium cells, such as TDKs, and the nutrient absorption functional genes in the BCs, particularly *SLC16A1*, responded to the changed rumen

fermented grass and its associated rumen microbiome. These changed grass-rumen functions affect the host bile acid profiles and amino acid metabolism. These findings deepen our understanding of the rumen function and its implications for optimizing grazing ruminant productivity, ecosystem stability, and grassland grazing sustainability. Further research is essential to assess the broader ecological impacts, including potential crosstalk between the rumen microbiome and host epithelial cells that may influence gene expression, forage intake, and systemic metabolism.

Methods

Animal experimental design and sampling

The experiment was conducted from July to September 2022 at Team 9 of Ternihe Ranch, Chenbalhu Banner, Hulunbuir League, Inner Mongolia Autonomous Region, an area characterized by temperate meadow grasslands and an annual precipitation of approximately 400 mm. Seventy-two healthy, three-month-old weaned Hulunbuir male lambs of similar size and weight (23.70 ± 1.22 kg) were selected for the study (ethics approval number AW52603202-5–1). The experiment employed a 2*3 two-factor randomized block design, with factors including grazing intensity and concentrate supplementation levels. Grazing intensity, which in this experiment was formulated according to the Evaluating criterion for balance of forage supply and livestock requirement (LY/T 3320–2022) published by the National Forestry and Grassland Administration, and was classified into moderate grazing (grass utilization rate of 40%, block area of 0.4 ha, carrying capacity of 10 lambs/ha, MG) and heavy grazing (grass utilization rate of 80%, block area of 0.2 ha, carrying capacity of 20 lambs/ha, HG) based on the area of grazing plots and grass utilization rate. Calculation of forage intake was performed using the snap cage method [73]. Previous studies utilized ITS2 barcoding to identify nine forage grass species [74], including *Leymus chinensis* (LC), *Bromus inermis* (BI), *Artemisia tanacetifolia* (AT), *Astragalus adsurgens* (AA), *Carex duriuscula* (CD), *Potentilla bifurca* (PB), *Medicago falcata* (MF), *Plantago depressa* (PD), and *Poa pratensis* (PP). These plants represented over 95% of the total vegetation in terms of height and canopy cover. The absolute intake of each species was calculated by multiplying its proportional representation by the total forage intake. Concentrate supplementation levels were 0% (NS), 1% (LS), and 2% (HS) of body weight. The lambs in the treatment groups were given supplemental feeding daily at 16h00 and free access to water throughout the three-month trial period. The supplementary feed formulas are provided in Table S16 indicate that corn grain and its by-products (corn bran and corn germ meal) constitute 68.67% of the dry matter in the concentrate. Thus, six groups were conducted for animal experiment in this study: HGNS, HGLS, HGHS, MGNS, MGLS, and MGHS.

Blood samples were collected from the jugular vein of each lamb before feeding on the morning of the day before slaughter and then centrifuged at 3000 × g for 10 min to isolate the serum. At the end of the feeding period, all animals were slaughtered, and samples of rumen contents and rumen wall were collected. Rumen contents were collected from the ventral region of the rumen and immediately filtered through four layers of medical gauze to remove undigested fiber and particulate matter, yielding a homogenized fluid sample. This sample was quickly divided into portions: one was used immediately for pH measurement, while the remaining portions were stored in liquid nitrogen for the analysis of SCFAs and ammonia nitrogen (within 1 month), and multiomics studies (within 1.5 years). For the molecular and multiomics analysis, we selected two groups of moderate grazing plus 0% concentrate supplementation (MGNS) and moderate grazing plus 2% concentrate supplementation (MGHS) based on the animal phenotypes (Tables 1 and 2). And the systematic workflow and feature overview of this multiomics study was shown in Fig. 7, including rumen microbiome metagenomics and metatranscriptome ($n=6$), rumen and blood metabolomics ($n=8$), rumen tissue single-cell RNA sequencing ($n=3$).

Rumen fermentation characteristics

The pH of the rumen fluid was promptly measured using a calibrated Testo 205 pH meter (Testo, Germany) with automatic temperature compensation. Ammonia-N levels were measured according to previously published methods [75]. The pre-treatment steps for SCFAs are as follows: clarified rumen fluid samples were centrifuged to remove feed particles and impurities (5400 rpm × 10 min). Then, 1 mL of the centrifuged supernatant and 0.2 mL of 25% metaphosphoric acid solution containing the internal standard 2-ethylbutyric acid (2 EB) were accurately added to a 1.5 mL centrifuge tube, thoroughly mixed, and incubated in an ice-water bath for at least 30 min. A subsequent centrifugation (10,000 rpm × 10 min) was performed to remove protein precipitates, and the resulting supernatant was collected for further analysis. The SCFAs concentrations were determined using gas chromatography (Trace 1300; Thermo Fisher Scientific Co., Ltd., Shanghai, China).

Metabolomics analysis

For the rumen fluid and serum samples, 100 μL of serum was mixed with 400 μL of an extraction solution (methanol: acetonitrile, 1:1, v/v) containing deuterated internal standards. The mixture was vortexed for 30 s,

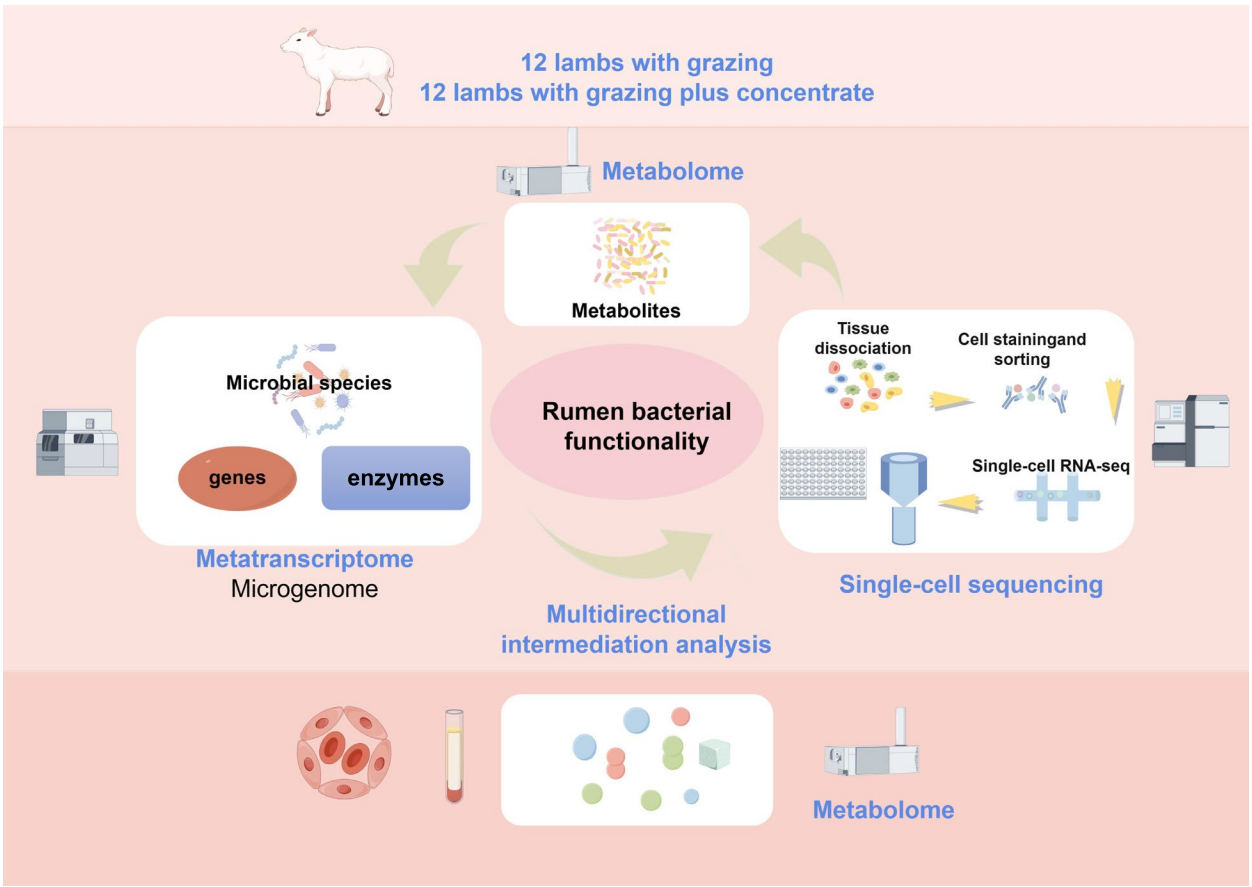

Fig. 7 A systematic workflow and pipeline overview of this study conducted with muti-omics on ruminal microbial metagenomics, metatranscriptomics, and metabolomics analysis, rumen epithelium single cell RNA-seq analysis, and host serum metabolomics, as well as their functional integrative analysis. This figure was drawn by Figdraw (ID: POOYI4b36f)

sonicated for 10 min in a 4 °C water bath, and incubated for 1 h at − 40 °C to precipitate proteins. The samples were then centrifuged at 13,800 × g for 15 min at 4 °C. The supernatant was transferred to a fresh glass vial for analysis. A quality control (QC) sample was prepared by mixing equal aliquots of the supernatants from all samples. Liquid chromatography-tandem mass spectrometry (LC–MS/MS) was performed using an ultra-high-performance liquid chromatography (UHPLC) system (Vanquish, Thermo Fisher Scientific) equipped with a Waters ACQUITY UPLC BEH Amide column (2.1 mm × 50 mm, 1.7 μm) and coupled to an Orbitrap Exploris 120 mass spectrometer (Orbitrap MS, Thermo). The mobile phase consisted of 25 mmol/L ammonium acetate and 25 mmol/L ammonia hydroxide in water (pH = 9.75) as solvent A, and acetonitrile as solvent B. The auto-sampler was maintained at 4 °C, and the injection volume was 2 μL. The Orbitrap Exploris 120 mass spectrometer was operated in information-dependent acquisition (IDA) mode, controlled by Xcalibur software (Thermo), continuously evaluating the full scan MS spectrum. The electrospray ionization (ESI) source conditions were as follows: sheath gas flow rate of 50 Arb, aux gas flow rate of 15 Arb, capillary temperature of 320 °C, full MS resolution of 60,000, MS/MS resolution of 15,000, collision energy of 20/30/40 (SNCE), and spray voltage of 3.8 kV (positive mode) or − 3.4 kV (negative mode).

Rumen microbiome metagenomics analysis

Microbial genomic DNA was extracted from 250 μL of homogenized liquid-phase subsample, a volume optimized to yield consistent DNA amounts (≥ 1 μg/sample, quantified by Qubit). Extraction involved bead-beating homogenization (500 mg of 0.1 mm glass beads) in 700 μL SLX-Plus Lysis Buffer with vortexing (2500 rpm, 10 min). After adding 70 μL DS precipitation buffer, samples were incubated at 70 °C for 10 min and centrifuged (12,000 × g, 5 min). The resulting supernatant (500 μL) underwent silica-binding

with SP2 Binding Buffer (170 µL) and HTR Reagent (170 µL) on ice (5 min). Clarified lysate (450 µL) was then purified magnetically using MagSi beads (40 µL) and sequential washes with XP5 Wash Buffer (500 µL), PHB (800 µL), and ethanol-SPM (800 µL, 1:1 v/v). DNA was air-dried for 15 min and eluted using pre-heated buffer (50–100 µL, 70 °C). Transfer the cleared supernatant containing purified DNA to a new 1.5 mL tube. The quantity and quality of the extracted DNA were assessed using a Qubit™ 4 Fluorometer (Invitrogen, USA) and agarose gel electrophoresis. Metagenomic libraries were constructed using the Illumina TruSeq Nano DNA LT Library Preparation Kit (Illumina, USA) with an insert size of ~ 400 bp. Each library was sequenced on the Illumina NovaSeq platform (Illumina, USA) using the paired-end 150 bp (PE150) strategy at Personal Biotechnology Co., Ltd. (Shanghai, China). Raw sequencing reads were processed to obtain high-quality reads for further analysis. First, sequencing adapters were removed using Cutadapt (v1.2.1) [76]. Second, low-quality reads were trimmed using the sliding-window algorithm in fastp (v0.23.2) [77], to remove host DNA contamination. The resulting quality-filtered reads were then used for taxonomical classification using Kraken2 (v2.0.8-beta) [78], against a GTDB-derived database that included archaeal and bacterial genomes from the GTDB database, viral sequences from the RVDB database, and eukaryotic microbial sequences from the NCBI-nt database. Reads assigned to metazoans or viridiplantae were excluded from downstream analyses.

For assembly, Megahit (v1.1.2) [79] was used with meta-large preset parameters. The resulting contigs (longer than 300 bp) were pooled and clustered using mmseqs2 [80] in "easy-linclust" mode, with a sequence identity threshold of 95% and a coverage threshold of 90% for the shorter contig. The lowest common ancestor taxonomy of non-redundant contigs was determined by aligning them against the NCBI-nt database using mmseqs2 in "taxonomy" mode. Contigs assigned to Viridiplantae or Metazoa were excluded from further analysis. Gene prediction in the contigs was performed using Prodigal (v2.6.3) [80]. The Coding Sequences (CDS) from all samples were clustered using mmseqs2 with the "easy-cluster" mode, with a protein sequence identity threshold of 95% and 90% coverage for the shorter contig. To assess gene abundances, high-quality reads from each sample were mapped to the predicted gene sequences using Minimap2, and feature Counts was used to count the aligned reads, yielding the Reads Count (RC) [81] for each gene. Finally, using the cluster corresponding file generated by gene deduplication, the RC of non-redundant proteins was obtained. The filtered protein sequence set was then compared with commonly used protein databases to annotate and analyze the gene functions across all samples. The comparison was performed using the search module of MMseqs2, with a sensitivity parameter set to 5.7. The predicted protein sequences were annotated based on the Carbohydrate-Active Enzymes database (CAZy database, version 2024–05) using the dbCAN2 meta-server (v2.0.11).

Rumen microbiome metatranscriptome

Total RNA was extracted using the RNA PowerSoil® Total RNA Isolation Kit (12,866–25) (MoBio, USA) according to the manufacturer's instructions. The quality and quantity of the extracted RNA were assessed using 1.5% agarose gel electrophoresis and a UV spectrophotometer. Additionally, RNA integrity (RIN ≥ 5.5) was verified using an Agilent 2100 Bioanalyzer (Agilent, USA). Following the removal of ribosomal RNA to isolate microbial RNA, cDNA synthesis and metatranscriptome library construction were performed using Illumina's TruSeq Stranded mRNA LT Sample Prep Kit (Illumina, USA). Libraries were sequenced on the Illumina NovaSeq platform (Illumina, USA) using the paired-end 150 bp (PE150) strategy at Personal Biotechnology Co., Ltd. (Shanghai, China).

Raw sequencing reads were processed to obtain high-quality reads for downstream analysis. The processing steps included (1) adapter removal: sequencing adapters were removed using Cutadapt (v1.17) [76]; (2) quality trimming: low-quality reads were trimmed using a sliding-window algorithm in fastp (v0.20.0) [82]; (3) host contamination removal: reads were aligned to the lamb genome using BMTagger to remove host contamination [83]; and (4) ribosomal RNA removal: ribosomal RNA sequences were removed using SortMeRNA (v4.2.0) [84] with its default rRNA reference database. After obtaining quality-filtered reads, taxonomical classifications of the metatranscriptomic reads were performed using Kraken2 [78] against a RefSeq-derived database. Reads assigned to metazoans or viridiplantae were excluded from downstream analyses. For assembly, Trinity (v2.11.0) [85] was used to assemble the reads for each sample. The resulting contigs (longer than 200 bp) were pooled and clustered using mmseqs2 [80] in "easy-linclust" mode, with a sequence identity threshold of 98% and 95% coverage for the shorter contig. The lowest common ancestor taxonomy of the non-redundant contigs was determined by aligning them against the NCBI-nt database using BLASTN.

Gene prediction in the contigs was performed using TransGeneScan (v1.3.0) [86]. The CDS of all samples were translated into proteins and further clustered

using mmseqs2 [80] in "cluster" mode, with a protein sequence identity threshold of 95% and 90% coverage for the shorter sequence. To quantify gene abundance, high-quality reads from each sample were mapped to the predicted gene sequences using Salmon [87] in quasi-mapping-based mode with "–meta–minScoreFraction = 0.55". The gene abundance was normalized using transcripts per kilobase per million mapped reads (TPM). The functionality of the non-redundant genes was annotated using mmseqs2 [80] in "search" mode against protein databases including KEGG and CAZy. KO were obtained using KOBAS [88].

Rumen tissue collection, dissociation and single-cell RNA sequencing

Three lambs from each experimental group were selected randomly for scRNA-seq. Epithelial tissues from the ventral bursa region of the rumen were collected post-slaughter, washed with saline to remove digestive fluids, and stored in liquid nitrogen for 1.5 years prior to further analysis. Rumen wall (abdominal sac) (0.25 g) was rinsed with pre-cooled sterile saline to remove feed particles and unattached microorganisms, and prepared by absorbing residual liquid, placing the tissues in sterile petri dishes, and chopping them into 1–2 mm3 pieces on ice. The pieces were transferred to freezing tubes, frozen in liquid nitrogen for 5 min, and stored in an ultra-low temperature freezer. A quality control (QC) sample was similarly prepared but frozen without chopping. Before nucleus isolation, the QC sample was thawed, and RNA was extracted to confirm integrity.

Nucleus isolation and purification involved transferring frozen tissue to a Dounce homogenizer, adding 500 µL of pre-cooled lysis buffer, thawing, and homogenizing the tissue with a loose pestle (15–20 strokes) followed by a tight pestle (5–10 strokes); the homogenate was then mixed with 700 µL of Nuclear Wash Buffer, filtered through a 70 µm strainer into a 50 mL tube, and combined with 1 mL of 50% iodixanol before preparing a gradient in a 15 mL tube with 33% and 30% iodixanol, layering the nuclei solution on top, and centrifuging at 10,000 × g for 20 min at 4 °C; the nuclei layer was collected from the 33%/30% iodixanol interface, washed with Nuclear Wash Buffer, filtered through a 40 µm filter, centrifuged again, and finally resuspended in 100 µL of Nuclear Wash Buffer; the nuclei suspension was stained with Trypan blue, counted under a microscope, and adjusted to a concentration of 700–1200 nuclei/µL using PBS as needed.

The library construction was performed according to the manufacturer's instructions. The Single Cell 5′ Protocol produced Illumina-ready sequencing libraries. A Single Cell 5′ Library comprised standard Illumina paired-end constructs which begin and end with P5 and P7. The Single Cell 5′ 16 bp 10 × Barcode and 10 bp UMI were encoded in Read 1, while Read 2 was used to sequence the cDNA fragment. Sample index sequences were incorporated as the i7 index read. Read 1 and Read 2 were standard Illumina® sequencing primer sites used in paired-end sequencing.

ScRNA-seq data processing, cell clustering, and cell type annotation

10X Genomics Cell Ranger software (version 3.1.0) was used to convert raw BCL files to FASTQ files, alignment, and counts quantification. Data quality control and genome alignment were performed according to manufacturer's instructions. Briefly, reads with low-quality barcodes and UMIs were filtered out and then mapped to the reference genome. Reads uniquely mapped to the transcriptome and intersecting an exon at least 50% were considered for UMI counting. Before quantification, the UMI sequences were corrected for sequencing errors, and valid barcodes were identified based on the EmptyDrops method [89]. The cell by gene matrices were produced via UMI counting and cell barcodes calling. The cell by gene matrices for each sample were individually imported to Seurat [90] version 3.1.1 for downstream analysis. Seurat implements a graph-based clustering approach. Distances between the cells were calculated based on previously identified PCs. Briefly, Seurat embed cells in a shared-nearest neighbor (SNN) graph, with edges drawn between cells via similar gene expression patterns. To partition this graph into highly interconnected quasi-cliques or communities, we first constructed the SNN graph based on the Euclidean distance in PCA space and refined the edge weights between any two cells based on the shared overlap in their local neighborhoods (Jaccard distance). We then clustered cells using the Louvain [91] method to maximize modularity. Regarding cell type annotation, we identified marker genes based on the specificity of the genes in the cell and their expression (≥ 50%) of all genes, and then compared the corresponding databases and several peer-reviewed single-cell transcriptomics studies in relevant animal systems [16, 56–58, 92] to identify the cells. The following three animal databases were mainly included:
CellMarker: http://117.50.127.228/CellMarker/;
Cell Taxonomy: https://ngdc.cncb.ac.cn/celltaxonomy/;
Cancer Single-cell Expression Map: https://ngdc.cncb.ac.cn/cancerscem/;

Expression values of each gene in given cluster were compared against the rest of cells using. The Wilcoxon rank sum test [93], significantly upregulated genes were identified using 3 criteria. First, genes had to be at least 1.28-fold overexpressed in the target cluster. Second, genes had to be expressed in more than 25% of the cells belonging to the target cluster. Third, P value had to be less than 0.05.

Based on the results of cell subpopulation classification, t-SNE plots were employed to visualize distinct cell subpopulation types. t-SNE (t-distributed stochastic neighbor embedding) is a probabilistic nonlinear dimensionality reduction method. Its primary objective is to map high-dimensional data into a low-dimensional space while preserving the local structural relationships between data points as much as possible.

Statistical analysis

Initial data organization and checks were performed using Microsoft Excel 2019, covering production performance, feed intake, and rumen fermentation parameters. Linear mixed modeling (IBM SPSS 26.0, USA) was used to analyze the performance indicators under two different grazing intensities and three levels of supplemental feeding, including live weight before slaughter, carcass weight, slaughter rate, ADG, and feed intake. The statistical model followed the approach outlined in our previous study as follows [94].

$$y_{ijkl} = \beta_0 + \alpha_i + \gamma_i + (\alpha\gamma)_{ij} + b_k + r_l(k) + \epsilon_{ijkl}$$

where y_{ijkl} is the dependent variable; β_0 is the overall mean; α_i is the effect of grazing intensity; γ_i is the effect of level of supplemental feeding; $(\alpha\gamma)_{ij}$ is the interaction between grazing intensity and level of supplemental feeding; b_k is the random effect of plot; $r_l(k)$ is the random effect of lamb; and ϵ_{ijkl} is the residual.

Then statistical of feed intake and rumen fermentation parameters between the MGHS and MGNS groups were performed using the unpaired Student's T tests in GraphPad Prism 9.5.0, with a significance level of $Q < 0.05$ (Benjamini–Hochberg adjusted $P < 0.05$). Prior to analysis, the normality of data distribution was confirmed via Shapiro–Wilk tests ($P > 0.05$), and homogeneity of variances was verified using F tests ($P > 0.05$). Results were considered statistically significant at a Benjamini–Hochberg adjusted $P < 0.05$ to control for false discovery rate (FDR) in multiple comparisons. For metagenomics and metatranscriptomics statistics data, linear discriminant analysis effect size (LEfSe) was performed to detect differentially abundant taxa and functions across groups using the default parameters. Alpha diversity was characterized using the Chao1 and Observed species indices to represent richness, the Shannon and Simpson indices to represent diversity, the Pielou's evenness index to represent evenness, and the Good's coverage index (Good, 1953) to represent coverage. Beta diversity analysis was performed to investigate the compositional and functional variation of microbial communities across samples using Bray–Curtis distance metrics and visualized via principal coordinate analysis (PCoA), nonmetric multidimensional scaling (NMDS). Additionally, the Adonis test (also known as PERMANOVA, permutational multivariate analysis of variance) was applied to assess statistical significance ($P < 0.05$). The analysis of rumen and serum metabolites, the value of variable importance in the projection (VIP) of the first principal component in OPLS-DA analysis was obtained. OPLS-DA models were constructed using one predictive component (focusing on between-group variation) and one orthogonal component (capturing within-group variation). The VIP values were calculated exclusively from the predictive component, as orthogonal components are intentionally designed to filter out variance unrelated to the class discrimination. This approach ensures that VIP scores reflect metabolites truly associated with the experimental groups. It summarizes the contribution of each variable to the model. The metabolites with VIP > 1 and $P < 0.05$ (student t test) were considered as significantly changed metabolites between the MGHS and MGNS group. ROC analysis was used to identify key metabolites markers. In addition, commercial databases including KEGG (http://www.genome.jp/kegg/) and MetaboAnalyst (http://www.metaboanalyst.ca/) were used for pathway enrichment analysis.

Supplementary Information

The online version contains supplementary material available at https://doi.org/10.1186/s40168-025-02200-z.

Supplementary Material 1: Table S1. Comparison of production performance between MGNS and MGHS lambs. Table S2. Proportion of short-chain fatty acids in rumen fluid of MGNS and MGHS lambs ($Q<0.05$). Table S3. Rumen differential metabolites between MGNS and MGHS lambs ($Q<0.05$). Table S4. Receiver operating characteristic (ROC) analysis of top ten up-regulated rumen metabolites. Table S5. Receiver operating characteristic (ROC) analysis of top ten down-regulated rumen metabolites. Table S6.Rumen differential metabolites between MGNS and MGHS lambs ($P<0.05$). . Table S7. Summary of metagenomics sequence data generated from rumen samples of 12 lambs. Table S8. Top 10 most abundant phyla in rumen microbiome. Table S9. Top 10 most abundant genera in rumen microbiome. Table S10. Summary of meta-transcriptomics sequence data generated from rumen samples of 12 lambs. Table S11. Serum differential metabolites between MGNS and MGHS lambs ($Q<0.05$). Table S12. Receiver operating characteristic (ROC) analysis of top ten up-regulated serum metabolites. Table S13. Receiver operating characteristic (ROC) analysis of top ten down-regulated serum metabolites. Table S14. Serum differential metabolites between MGNS and MGHS lambs ($P<0.05$). Table S15. Microorganisms with differences in macrogenic and macrotranscriptional analysis. Table S16. The ingredients and nutrients composition of supplemental feeding diet.

Supplementary Material 2: Figure S1. A Alpha diversity. B Differences in family levels by metagenome sequencing. Figure S2. A The distribution of PL among the top 20 genera. B The distribution of CMB among the top 20 genera. Figure S3. A Metabolic pathway analysis bubble diagram of differentiated keratinocytes (DKs). B Metabolic pathway analysis bubble diagram of terminally differentiated keratinocytes (TDKs). Figure S4. The classification of differential serum metabolite.

Acknowledgements
We thank all the members from our Laboratory participation for the animal feeding studies and sampling. We are grateful to Shanghai Biotree Biotech Co., Ltd. for providing help in metabolomics analysis, Personal Biotechnology Co., Ltd. (Shanghai, China) for providing help in metagenomics and metatranscriptomics analysis, and the single cell sequencing platform and bioinformation analysis of Gene Denovo Biotechnology Co., Ltd (Guangzhou, China).

Authors'contributions
The overall experiment was designed by HLL, YJZ and NL. XHM and BW wrote the manuscript and conducted the data analysis, and HLL reviewed it. Feeding trials were conducted by MLX. XHM, ZL, HY, LT, XMX, BZ, ZW, YTW, JGL, and JB participated in the animal feeding, sampling, and samples analysis. All authors read and approved the final version of the manuscript.

Funding
This project was supported by grants from the Major Program of National Natural Science Foundation of China (32192463).
The Major Program of National Natural Science Foundation of China,32192463
The rumen metagenomic data from this study were uploaded to the NCBI Sequence Read Archive (SRA) under the accession numbers PRJNA1162000. The metatranscriptomics data were deposited into the NCBI SRA under the accession numbers PRJNA1164963.The raw data of the rumen epithelium generated in this study were deposited into the NCBI SRA under the accession numbers PRJNA1164898. The processed sequencing data of the rumen epithelium have been submitted to the NCBI Gene Expression Omnibus (GEO; GSE278012).

Data availability
Availability of data and materials The rumen metagenomic data from this study were uploaded to the NCBI Sequence Read Archive(SRA) under the accession numbers PRJNA1162000. The metatranscriptomics data were deposited into the NCBI SRA under the accession numbers PRJNA1164963.The raw data of the rumen epithelium generated in this study were deposited into the NCBI SRA under the accession numbers PRJNA1164898. The processed sequencing data of the rumen epithelium have been submitted to the NCBI Gene Expression Omnibus (GEO; GSE278012).

Declarations

Ethics approval and consent to participate
All experimental procedures involving animals adhered to ethical guidelines and were approved by the Animal Care Committee of China Agricultural University (Beijing, China; approval no. AW52603202-5–1).

Consent for publication
Not applicable.

Competing interests
The authors declare no competing interests.

Author details
[1]State Key Laboratory of Animal Nutrition and Feeding, College of Animal Science and Technology, China Agricultural University, Beijing 100193, People's Republic of China. [2]College of Grass Science and Technology, China Agricultural University, Beijing 100193, People's Republic of China.

Received: 27 September 2024 Accepted: 11 July 2025
Published online: 12 December 2025

References

1. He M, Pan Y, Zhou G, Barry KE, Fu Y, Zhou X. Grazing and global change factors differentially affect biodiversity-ecosystem functioning relationships in grassland ecosystems. Global Change Biol. 2022;28(18):5492–504. https://doi.org/10.1111/gcb.16305.
2. Fajardo NM, Poli CHEC, Bremm C, Tontini JF, Castilhos ZMS, McManus CM, et al. Effect of concentrate supplementation on performance and ingestive behaviour of lambs grazing tropical Aruana grass (*Panicum maximum*). Anim Prod Sci. 2016;56(10):1693–9. https://doi.org/10.1071/AN14698.
3. Faisca LD, Peres MTP, Fernandes SR, Bonnet OJF, Batista R, Deiss L, et al. A new insight about the selection and intake of forage by ewes and lambs in different production systems on pasture. Small Rumin Res. 2023;221:106949. https://doi.org/10.1016/j.smallrumres.2023.106949.
4. Huang Y, Zhao M, Zhang X, Wei H, Liu L, Zhang Z, et al. Indoor feeding combined with restricted grazing time improves body health, slaughter performance, and meat quality in Huang-huai sheep. Anim Biosci. 2023;36(11):1655–65. https://doi.org/10.5713/ab.23.0252.
5. de Menezes AB, Lewis E, O'Donovan M, O'Neill BF, Clipson N, Doyle EM. Microbiome analysis of dairy cows fed pasture or total mixed ration diets. FEMS Microbiol Ecol. 2011;78(2):256–65. https://doi.org/10.1111/j.1574-6941.2011.01151.x.
6. Henderson G, Cox F, Ganesh S, Jonker A, Young W, Abecia L, et al. Rumen microbial community composition varies with diet and host, but a core microbiome is found across a wide geographical range. Scie Rep. 2015;5(1):14567. https://doi.org/10.1038/srep14567.
7. Cui X, Wang Z, Guo P, Li F, Chang S, Yan T, et al. Shift of feeding strategies from grazing to different forage feeds reshapes the rumen microbiota to improve the ability of Tibetan sheep (Ovis aries) to adapt to the cold season. Microbiol Spectrum. 2023;11(2): e02816. https://doi.org/10.1128/spectrum.02816-22.
8. Thomas M, Webb M, Ghimire S, Blair A, Olson K, Fenske GJ, et al. Metagenomic characterization of the effect of feed additives on the gut microbiome and antibiotic resistome of feedlot cattle. Sci Rep. 2017;7(1):12257. https://doi.org/10.1038/s41598-017-12481-6.
9. Hao Y, Hao S, Andersen-Nissen E, Mauck WM 3rd, Zheng S, Butler A, et al. Integrated analysis of multimodal single-cell data. Cell. 2021;184(13):3573-87.e29. https://doi.org/10.1016/j.cell.2021.04.048.
10. Shinkai T, Mitsumori M, Sofyan A, Kanamori H, Sasaki H, Katayose Y, et al. Comprehensive detection of bacterial carbohydrate-active enzyme coding genes expressed in cow rumen. Anim Sci J. 2016;87(11):1363–70. https://doi.org/10.1111/asj.12585.
11. Comtet-Marre S, Parisot N, Lepercq P, Chaucheyras-Durand F, Mosoni P, Peyretaillade E, et al. Metatranscriptomics reveals the active bacterial and eukaryotic fibrolytic communities in the rumen of dairy cow fed a mixed diet. Front Microbiol. 2017;8:67. https://doi.org/10.3389/fmicb.2017.00067.
12. Peixoto RS, Harkins DM, Nelson KE. Advances in microbiome research for animal health. Annu Rev Anim Biosci. 2021;9:289–311. https://doi.org/10.1146/annurev-animal-091020-075907.
13. Flint HJ, Bayer EA. Plant cell wall breakdown by anaerobic microorganisms from the Mammalian digestive tract. Ann N Y Acad Sci. 2008;1125:280–8. https://doi.org/10.1196/annals.1419.022.
14. Steele MA, Penner GB, Chaucheyras-Durand F, Guan LL. Development and physiology of the rumen and the lower gut: Targets for improving gut health. J Dairy Sci. 2016;99(6):4955–66. https://doi.org/10.3168/jds.2015-10351.
15. Jiao J, Huang J, Zhou C, Tan Z. Taxonomic identification of ruminal epithelial bacterial diversity during rumen development in goats. Appl Environ Microbiol. 2015;81(10):3502–9. https://doi.org/10.1128/aem.00203-15.
16. Gao Y, Fang L, Baldwin RLt, Connor EE, Cole JB, Van Tassell CP, et al. Single-cell transcriptomic analyses of dairy cattle ruminal epithelial cells during weaning. Genomics. 2021;113(4):2045–55. https://doi.org/10.1016/j.ygeno.2021.04.039.
17. Yan Y, Zhu S, Jia M, Chen X, Qi W, Gu F, et al. Advances in single-cell transcriptomics in animal research. Journal of animal science and biotechnology. 2024;15(1):102. https://doi.org/10.1186/s40104-024-01063-y.
18. Shalek AK, Satija R, Shuga J, Trombetta JJ, Gennert D, Lu D, et al. Single-cell RNA-seq reveals dynamic paracrine control of cellular variation. Nature. 2014;510(7505):363–9. https://doi.org/10.1038/nature13437.

19. Li Y, Mao K, Zang Y, Lu G, Qiu Q, Ouyang K, et al. Revealing the developmental characterization of rumen microbiome and its host in newly received cattle during receiving period contributes to formulating precise nutritional strategies. Microbiome. 2023;11(1):238. https://doi.org/10.1186/s40168-023-01682-z.
20. Seddik H, Xu L, Wang Y, Mao SY. A rapid shift to high-grain diet results in dynamic changes in rumen epimural microbiome in sheep. Animal. 2019;13(8):1614–22. https://doi.org/10.1017/S1751731118003269.
21. Forbes TDA. Researching the Plant-Animal Interface: The investigation of Ingestive Behavior in Grazing Animals. J Anim Sci. 1988;66(9):2369–79. https://doi.org/10.2527/jas1988.6692369x.
22. Dineen M, McCarthy B, Dillon P, Coughlan F, Galvin N, Van Amburgh ME. The effect of concentrate supplement type on milk production, nutrient intake, and total-tract nutrient digestion in mid-lactation, spring-calving dairy cows grazing perennial ryegrass (Lolium perenne L.) pasture. J Dairy Sci. 2021;104(11):11593–608. https://doi.org/10.3168/jds.2021-20148.
23. Reis RB, Combs DK. Effects of increasing levels of grain supplementation on rumen environment and lactation performance of dairy cows grazing grass-legume pasture. J Dairy Sci. 2000;83(12):2888–98. https://doi.org/10.3168/jds.S0022-0302(00)75189-7.
24. Matejovsky KM, Sanson DW. Intake and digestion of low-, medium-, and high-quality grass hays by lambs receiving increasing levels of corn supplementation. J Anim Sci. 1995;73(7):2156–63. https://doi.org/10.2527/1995.7372156x.
25. Soder KJ, Thomas VM, Kott RW, Hatfield PG, Olson B. Influence of energy or protein supplementation during midpregnancy on forage intake of ewes grazing Montana winter range. J anim sci. 1995;73(10):2853–9. https://doi.org/10.2527/1995.73102853x.
26. Krysl L, Hess B. Influence of supplementation on behavior of grazing cattle. J Anim Sci. 1993;71(9):2546–55. https://doi.org/10.2527/1993.7192546x.
27. Wang Y, Wan H, Hu Z, Gao J, Sun C, Yang B. Artemisia Frigida Distribution Mapping in Grassland with Unmanned Aerial Vehicle Imagery and Deep Learning. Drones. 2024;8(4):151. https://doi.org/10.3390/drones8040151.
28. Zhang H, Liu N, Yang GW, Badgery WB, Guo YP, Zhang YJ. Diet selection of sheep shifted from quality to quantity characteristics of forages as sward availability decreased. Animal. 2022;16(6): 100546. https://doi.org/10.1016/j.animal.2022.100546.
29. Nishihara K, van Niekerk J, Innes D, He Z, Cánovas A, Guan LL, et al. Transcriptome profiling revealed that key rumen epithelium functions change in relation to short-chain fatty acids and rumen epithelium-attached microbiota during the weaning transition. Genomics. 2023;115(5): 110664. https://doi.org/10.1016/j.ygeno.2023.110664.
30. Ragaller V, Lebzien P, Südekum KH, Hüther L, Flachowsky G. Pantothenic acid in ruminant nutrition: a review. Journal of animal physiology and animal nutrition. J Anim Physiol Anim Nutr (Berl). 2011;95(1):6–16. https://doi.org/10.1111/j.1439-0396.2010.01004.x
31. Schwab EC, Schwab CG, Shaver RD, Girard CL, Putnam DE, Whitehouse NL. Dietary forage and nonfiber carbohydrate contents influence B-vitamin intake, duodenal flow, and apparent ruminal synthesis in lactating dairy cows. J Dairy Sci. 2006;89(1):174–87. https://doi.org/10.3168/jds.S0022-0302(06)72082-3.
32. Ma Y, Bao Y, Wang S, Li T, Chang X, Yang G, et al. Anti-inflammation effects and potential mechanism of saikosaponins by regulating nicotinate and nicotinamide metabolism and arachidonic acid metabolism. Inflammation. 2016;39(4):1453–61. https://doi.org/10.1007/s10753-016-0377-4.
33. Zhou Z, Chen J, Cui Y, Zhao R, Wang H, Yu R, et al. Antihypertensive activity of different components of Veratrum alkaloids through metabonomic data analysis. Phytomedicine. 2023;120: 155033. https://doi.org/10.1016/j.phymed.
34. Raza SHA, Naqvi SRZ, Abdelnour SA, Schreurs N, Mohammedsaleh ZM, Khan I, et al. Beneficial effects and health benefits of Astaxanthin molecules on animal production: A review. Res Vet Sci. 2021;138:69–78. https://doi.org/10.1016/j.rvsc.2021.05.023.
35. Chen G. 2, 6-cyclolycopene-1, 5-diol: A new marker of oxidative stress. Wayne State University; 2002.
36. Chai J, Weiss CP, Beck PA, Zhao W, Li Y, Zhao J. Diet and monensin influence the temporal dynamics of the rumen microbiome in stocker and finishing cattle. J Anim Sci and Biotechnol. 2024;15(1):12. https://doi.org/10.1186/s40104-023-00967-5.
37. Brulc JM, Yeoman CJ, Wilson MK, Berg Miller ME, Jeraldo P, Jindou S, et al. Cellulosomics, a gene-centric approach to investigating the intraspecific diversity and adaptation of Ruminococcus flavefaciens within the Rumen. PLoS ONE. 2011;6(10): e25329. https://doi.org/10.1371/journal.pone.0025329.
38. Liang J, Lv L, Sun L, Chen L, Zhang G, Zhang P. Metagenomic analysis reveals the community composition and functional characteristics of ruminal microbes in fermenting lignocellulosic biomass in vivo and in vitro. J Environ Chem Eng. 2025;13(2): 115851. https://doi.org/10.1016/j.jece.2025.115851.
39. Li F, Guan LL. Metatranscriptomic profiling reveals linkages between the active rumen microbiome and feed efficiency in beef cattle. Appl Environ Microbiol. 2017;83(9):e00061-e117. https://doi.org/10.1128/AEM.00061-17.
40. Biddle A, Stewart L, Blanchard J, Leschine S. Untangling the genetic basis of fibrolytic specialization by Lachnospiraceae and Ruminococcaceae in diverse gut communities. Diversity. 2013;5(3):627–40. https://doi.org/10.3390/d5030627.
41. Gagen EJ, Padmanabha J, Denman SE, McSweeney CS. Hydrogenotrophic culture enrichment reveals rumen Lachnospiraceae and Ruminococcaceae acetogens and hydrogen-responsive Bacteroidetes from pasture-fed cattle. FEMS Microbiol Lett. 2015;362(14). https://doi.org/10.1093/femsle/fnv104.
42. Jiao J, Wu J, Zhou C, He Z, Tan Z, Wang M. Ecological niches and assembly dynamics of diverse microbial consortia in the gastrointestine of goat kids. Isme J. 2024;18(1). https://doi.org/10.1093/ismejo/wrae002.
43. Saenz JS, Seifert J, Rios-Galicia B. Antiviral defence systems in the rumen microbiome. BioRxiv. 2024:2024.04. 04.588093.
44. Sato Y, Takebe H, Oishi K, Yasuda J, Kumagai H, Hirooka H, et al. Identification of 146 Metagenome-assembled genomes from the rumen microbiome of cattle in Japan. Microbes and Environ. 2022;37(4):ME22039. https://doi.org/10.1264/jsme2.ME22039.
45. Yan M, Yu Z. Viruses contribute to microbial diversification in the rumen ecosystem and are associated with certain animal production traits. Microbiome. 2024;12(1):82. https://doi.org/10.1186/s40168-024-01791-3.
46. Sato Y, Sato R, Fukui E, Yoshizawa F. Impact of rumen microbiome on cattle carcass traits. Sci Rep. 2024;14(1):6064. https://doi.org/10.1038/s41598-024-56603-3.
47. Wylensek D, Hitch TC, Riedel T, Afrizal A, Kumar N, Wortmann E, et al. A collection of bacterial isolates from the pig intestine reveals functional and taxonomic diversity. Nat Commun. 2020;11(1):6389. https://doi.org/10.1038/s41467-020-19929-w.
48. Fernando SC, Purvis H, Najar F, Sukharnikov L, Krehbiel C, Nagaraja T, et al. Rumen microbial population dynamics during adaptation to a high-grain diet. Appl Environ Microbiol. 2010;76(22):7482–90. https://doi.org/10.1128/AEM.00388-10.
49. Firkins J, Yu Z. Ruminant nutrition symposium: how to use data on the rumen microbiome to improve our understanding of ruminant nutrition. J Anim Sci. 2015;93(4):1450–70. https://doi.org/10.2527/jas.2014-8754.
50. Rytioja J, Hildén K, Yuzon J, Hatakka A, de Vries RP, Mäkelä MR. Plant-polysaccharide-degrading enzymes from Basidiomycetes. Microbiol Mol Biol Rev. 2014;78(4):614–49. https://doi.org/10.1128/mmbr.00035-14.
51. Bourne Y, Henrissat B. Glycoside hydrolases and glycosyltransferases: families and functional modules. Curr Opin Struct Biol. 2001;11(5):593–600. https://doi.org/10.1016/s0959-440x(00)00253-0.
52. Martinez-Fleites C, Korczynska JE, Davies GJ, Cope MJ, Turkenburg JP, Taylor EJ. The crystal structure of a family GH25 lysozyme from Bacillus anthracis implies a neighboring-group catalytic mechanism with retention of anomeric configuration. Carbohyd Res. 2009;344(13):1753–7. https://doi.org/10.1016/j.carres.2009.06.001.
53. Dash A, Modak R. Protein acetyltransferases mediate bacterial adaptation to a diverse environment. J Bacteriol. 2021;203(19): e0023121. https://doi.org/10.1128/jb.00231-21.
54. Bohra V, Dafale NA, Purohit HJ. Understanding the alteration in rumen microbiome and CAZymes profile with diet and host through comparative metagenomic approach. Arch Microbiol. 2019;201(10):1385–97. https://doi.org/10.1007/s00203-019-01706-z.
55. Houfani AA, Tláskal V, Baldrian P, Hahnke RL, Benallaoua S. Actinobacterial strains as genomic candidates for characterization of genes encoding

enzymes in bioconversion of lignocellulose. Waste Biomass Valorization. 2022;13(3):1523–34. https://doi.org/10.1007/s12649-021-01595-8.
56. Yuan Y, Sun DM, Qin T, Mao SY, Zhu WY, Yin YY, et al. Single-cell transcriptomic landscape of the sheep rumen provides insights into physiological programming development and adaptation of digestive strategies. Zool Res. 2022;43(4):634–47. https://doi.org/10.24272/j.issn.2095-8137.2022.086.
57. Wu J-J, Zhu S, Gu F, Valencak TG, Liu J-X, Sun H-Z. Cross-tissue single-cell transcriptomic landscape reveals the key cell subtypes and their potential roles in the nutrient absorption and metabolism in dairy cattle. J Adv Res. 2022;37:1–18. https://doi.org/10.1016/j.jare.2021.11.009.
58. Xue MY, Wu JJ, Xie YY, Zhu SL, Zhong YF, Liu JX, et al. Investigation of fiber utilization in the rumen of dairy cows based on metagenome-assembled genomes and single-cell RNA sequencing. Microbiome. 2022;10(1):11. https://doi.org/10.1186/s40168-021-01211-w.
59. Na SW, Guan LL. Understanding the role of rumen epithelial host-microbe interactions in cattle feed efficiency. Anim Nutr. 2022;10:41–53. https://doi.org/10.1016/j.aninu.2022.04.002.
60. Xiang R, Oddy VH, Archibald AL, Vercoe PE, Dalrymple BP. Epithelial, metabolic and innate immunity transcriptomic signatures differentiating the rumen from other sheep and mammalian gastrointestinal tract tissues. Peer J. 2016;4: e1762. https://doi.org/10.7717/peerj.1762.
61. van Hasselt PM, Ferdinandusse S, Monroe GR, Ruiter JP, Turkenburg M, Geerlings MJ, et al. Monocarboxylate transporter 1 deficiency and ketone utilization. N Engl J Med. 2014;371(20):1900–7. https://doi.org/10.1056/NEJMoa1407778.
62. Hatt J-M, Codron D, Ackermans NL, Martin LF, Richter H, Kircher PR, et al. The effect of the rumen washing mechanism in sheep differs with concentration and size of abrasive particles. Palaeogeogr Palaeoclimatol, Palaeoecol. 2020;550: 109728. https://doi.org/10.1016/j.palaeo.2020.109728.
63. Ma L, Zhao M, Zhao LS, Xu JC, Loor JJ, Bu DP. Effects of dietary neutral detergent fiber and starch ratio on rumen epithelial cell morphological structure and gene expression in dairy cows. J Dairy Sci. 2017;100(5):3705–12. https://doi.org/10.3168/jds.2016-11772.
64. Yang Y, Dong G, Wang Z, Wang J, Zhang Z, Liu J. Rumen and plasma metabolomics profiling by UHPLC-QTOF/MS revealed metabolic alterations associated with a high-corn diet in beef steers. PLoS ONE. 2018;13(11): e0208031. https://doi.org/10.1371/journal.pone.0208031.
65. Zhang R, Zhu W, Jiang L, Mao S. Comparative metabolome analysis of ruminal changes in Holstein dairy cows fed low- or high-concentrate diets. Metabolomics. 2017;13(6):74. https://doi.org/10.1007/s11306-017-1204-0.
66. Roeder T. Tyramine and octopamine: ruling behavior and metabolism. Annu Rev Entomol. 2005;50(1):447–77. https://doi.org/10.1146/annurev.ento.50.071803.130404.
67. Patel A, Thompson A, Abdelmalek L, Adams-Huet B, Jialal I. The relationship between tyramine levels and inflammation in metabolic syndrome. Horm Mol Biol Clin Invest. 2019;40(1). https://doi.org/10.1515/hmbci-2019-0047.
68. Lambert GW, Eisenhofer G, Jennings GL, Esler MD. Regional homovanillic acid production in humans. Life Sci. 1993;53(1):63–75. https://doi.org/10.1016/0024-3205(93)90612-7.
69. Lv R, Elsabagh M, Obitsu T, Sugino T, Kurokawa Y. Effect of phytol in forage on phytanic acid content in cow's milk. Anim Biosci. 2021;34(10):1616–22. https://doi.org/10.5713/ab.21.0086.
70. Hansen RP. Phytanic acid and other branched-chain fatty acid constituents of bovine rumen bacteria. J Dairy Res. 1966;33(3):333–42. https://doi.org/10.1017/S0022029900012024.
71. Wang B, Zhang B, Zhou L, Li S, Li Z, Luo H. Multi-omics reveals diet-induced metabolic disorders and liver inflammation via microbiota-gut-liver axis. J Nutr Biochem. 2023;111: 109183. https://doi.org/10.1016/j.jnutbio.2022.109183.
72. Lin L, Lai Z, Yang H, Zhang J, Qi W, Xie F, et al. Genome-centric investigation of bile acid metabolizing microbiota of dairy cows and associated diet-induced functional implications. ISME J. 2023;17(1):172–84. https://doi.org/10.1038/s41396-022-01333-5.
73. Zahran BB, Holm A, Stern WR, Loneragan W. The cage method of sampling to assess herbage mass and herbage consumed on annual rangeland vegetation. Rangeland J. 1988;10. https://doi.org/10.1071/RJ9880006.
74. Guo Y, Zhao X, Liu M, Zhang C, Zhang Y, Ma Q, et al. Using fecal DNA metabarcoding to investigate foraging reveals the effects of specific herbage on the improved n-3 fatty acid (PUFA) composition in the longissimus dorsi muscle of grazing tan sheep. J Agric Food Chem. 2021;69(33):9725–34. https://doi.org/10.1021/acs.jafc.1c03788.
75. Broderick G, Kang J. Automated simultaneous determination of ammonia and total amino acids in ruminal fluid and in vitro media. J Dairy Sci. 1980;63(1):64–75. https://doi.org/10.3168/jds.S0022-0302(80)82888-8.
76. Martin M. Cutadapt removes adapter sequences from high-throughput sequencing reads. EMBnet J. 2011;17(1):10–2. https://doi.org/10.1089/cmb.2017.0096.
77. Li H. Minimap2: pairwise alignment for nucleotide sequences. Bioinformatics. 2018;34(18):3094–100. https://doi.org/10.1093/bioinformatics/bty191.
78. Wood DE, Lu J, Langmead B. Improved metagenomic analysis with Kraken 2. Genome Biol. 2019;20:1–13. https://doi.org/10.1186/s13059-019-1891-0.
79. Li D, Liu C-M, Luo R, Sadakane K, Lam T-W. MEGAHIT: an ultra-fast single-node solution for large and complex metagenomics assembly via succinct de Bruijn graph. Bioinformatics. 2015;31(10):1674–6. https://doi.org/10.1093/bioinformatics/btv033.
80. Steinegger M, Söding J. MMseqs2 enables sensitive protein sequence searching for the analysis of massive data sets. Nat Biotechnol. 2017;35(11):1026–8. https://doi.org/10.1038/nbt.3988.
81. Liao Y, Smyth GK, Shi W. feature Counts: an efficient general purpose program for assigning sequence reads to genomic features. Bioinformatics. 2014;30(7):923–30. https://doi.org/10.1093/bioinformatics/btt656.
82. Chen S, Zhou Y, Chen Y, Gu J. fastp: an ultra-fast all-in-one FASTQ preprocessor. Bioinformatics. 2018;34(17):i884–90. https://doi.org/10.1093/bioinformatics/bty560.
83. Rotmistrovsky K, Agarwala R. BMTagger: Best Match Tagger for removing human reads from metagenomics datasets. NCBI/NLM, National Institutes of Health. 2011.
84. Kopylova E, Noé L, Touzet H. SortMeRNA: fast and accurate filtering of ribosomal RNAs in metatranscriptomic data. Bioinformatics. 2012;28(24):3211–7. https://doi.org/10.1093/bioinformatics/bts611.
85. Grabherr MG, Haas BJ, Yassour M, Levin JZ, Thompson DA, Amit I, et al. Full-length transcriptome assembly from RNA-Seq data without a reference genome. Nat Biotechnol. 2011;29(7):644–52. https://doi.org/10.1038/nbt.1883.
86. Ismail WM, Ye Y, Tang H. Gene finding in metatranscriptomic sequences. In: BMC bioinformatics. vol. 15: Springer; 2014: 1–8. https://doi.org/10.1186/1471-2105-15-S9-S8.
87. Patro R, Duggal G, Kingsford C. Salmon: accurate, versatile and ultrafast quantification from RNA-seq data using lightweight-alignment. BioRxiv. 2015;10: 021592. https://doi.org/10.1101/021592.
88. Bu D, Luo H, Huo P, Wang Z, Zhang S, He Z, et al. KOBAS-i: intelligent prioritization and exploratory visualization of biological functions for gene enrichment analysis. Nucleic Acids Res. 2021;49(W1):W317–25. https://doi.org/10.1093/nar/gkab447.
89. Lun ATL, Riesenfeld S, Andrews T, Dao TP, Gomes T, Marioni JC. EmptyDrops: distinguishing cells from empty droplets in droplet-based single-cell RNA sequencing data. Genome Biol. 2019;20(1):63. https://doi.org/10.1186/s13059-019-1662-y.
90. Butler A, Hoffman P, Smibert P, Papalexi E, Satija R. Integrating single-cell transcriptomic data across different conditions, technologies, and species. Nat Biotechnol. 2018;36(5):411–20. https://doi.org/10.1038/nbt.4096.
91. Rotta R, Noack A. Multilevel local search algorithms for modularity clustering. ACM J Exp Algorithmics. 2011;16:2.1–2.27. https://doi.org/10.1145/1963190.1970376.
92. Zhang K, Zhang Y, Qin J, Zhu H, Liu N, Sun D, et al. Early concentrate starter introduction induces rumen epithelial parakeratosis by blocking keratinocyte differentiation with excessive ruminal butyrate accumulation. J Adv Res. 2024;66:71–86. https://doi.org/10.1016/j.jare.2023.12.016.
93. Camp JG, Sekine K, Gerber T, Loeffler-Wirth H, Binder H, Gac M, et al. Multilineage communication regulates human liver bud development from

pluripotency. Nature. 2017;546(7659):533–8. https://doi.org/10.1038/nature22796.
94. Ji J, Yang H, Xu M, Zhang Y, Zhao X, Li Z, et al. DIA-based quantitative proteomic insight of lamb meat quality: tenderness and amino acid profile under different grazing intensities. LWT. 2025;215: 117285. https://doi.org/10.1016/j.lwt.2024.117285.

Publisher's Note